

9 OSCILLATIONS IN NONLINEAR SAMPLED-DATA SYSTEMS

9.0 INTRODUCTION

All the material of the preceding chapters has been concerned with systems which process signals *continuously* around the loop. This chapter takes under consideration the describing function analysis of nonlinear systems which at some point process *discrete samples* of signals. It should not come as a surprise that the analysis of nonlinear sampled-data systems is more complicated, or at least more laborious, than the corresponding analysis of nonlinear continuous-data systems. The treatment in this chapter considers just bias and single-sinusoid signals present at the input to the nonlinear part of the system. Even in the simplest case of a single sinusoid, the presence of another periodic process in the system—the sampling operation—gives rise to complications of the same kind as are encountered in the study of continuous systems with two sinusoidal components at the nonlinearity input. These complications are significant when the frequencies of the two periodic processes are rationally related, and this is the case of first importance in the study of nonlinear sampled-data systems.

Sampled-data systems have come into practical importance for a variety of reasons. The earliest of these had primarily to do with economy in the design and use of equipment. Many problems in impedance matching or power-level matching can be avoided if critical components are isolated—disconnected—most of the time, and the connection made only briefly at periodic intervals to read out a sample of the signal. The possibility of time-sharing one component among several systems also gives rise to a sampled form of signal processing. A major increase in interest in sampled-data systems was caused by the development of radar systems during the 1940s. Most radars provide information only in the form of periodic samples either because of a periodic scanning process or because of pulsed transmission of the microwave energy. A more recent surge of interest has been due to the increasing utilization of digital computers as controllers in feedback systems. In some areas of application, especially aerospace guidance and control, the use of discrete-data processors is often a practical necessity. Thus many system engineers find themselves concerned almost exclusively with the design of sampled-data systems. And as with continuous systems, these systems may be designed with, or otherwise may suffer from, a number of important nonlinear effects.

THE EFFECTS OF SAMPLING

In this chapter, as in most of the preceding material, attention is centered on systems which can be reduced to single-loop configurations having a single nonlinear part separated from the linear part. The linear part in this case may include any number of continuous linear elements and discrete, or pulsed, linear elements. The ordering of these elements around the loop is of some consequence to the application of describing function theory, because in this case higher-frequency, and possibly lower-frequency, components are generated, not only by the nonlinear part, but by the sampling operations as well. Consider the system configuration of Fig. 9.0-1a. In the study of steady-state oscillations in this system, the nonlinearity input, being the output of the continuous linear filter, may reasonably be taken as a sinusoid for the purpose of quasi-linearization. The output of the nonlinearity, $y(t)$, then contains harmonic components at the fundamental and higher harmonic frequencies. On a two-sided frequency scale, the harmonic components of $y(t)$ would in general have the frequencies $\pm k\omega$, $k = 0, 1, 2, \dots$, where ω is the frequency of the input sinusoid. The sampling operation modulates $y(t)$ with the frequencies $\pm l\omega_s$, $l = 0, 1, 2, \dots$, where ω_s is the frequency of closure of the sampling switch.¹ Thus $y^*(t)$ contains

¹ The reader who needs a basic treatment of the description of the sampling operation, the transfer of sampled signals through linear systems, and z-transform theory is directed to any one of a number of texts on the subject. Among them are Jury (Ref. 7), Kuo (Ref. 15), Raggazzini and Franklin (Ref. 22), and Tou (Ref. 27).

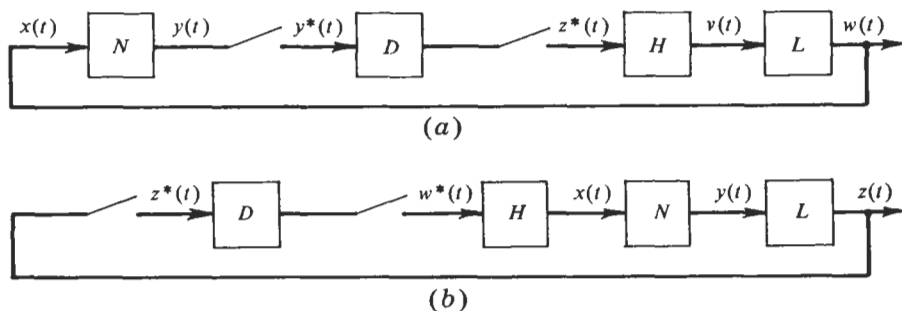


Figure 9.0-1 Nonlinear sampled-data system configurations. N = static nonlinear element; H = data hold; D = discrete linear element; L = continuous linear element. Asterisks denote sampled signals.

harmonic components with frequencies $\pm k\omega \pm l\omega_s$. These frequencies, which appear in the loop, determine to a large extent the possibility of successful application of describing function theory.

1. If the frequency ratio ω/ω_s is irrational, $y^*(t)$ is aperiodic. It contains a harmonic component with frequency ω ; in fact, that component is just $1/T_s$ times the fundamental component of the nonlinearity output. This may be seen from the familiar expression for the transform of $y^*(t)$:

$$Y^*(j\omega) = \frac{1}{T_s} \sum_{l=-\infty}^{\infty} Y[j(\omega + l\omega_s)] \quad (9.0-1)$$

If ω_s is not rationally related to ω , the only term in this sum with frequency ω is the primary term for $l = 0$. Thus, if describing function theory can be applied at all in the case of irrational frequencies, the describing function relating $x(t)$ to $y^*(t)$ is just $1/T_s$ times the ordinary single-sinusoid-input describing function for the nonlinearity which relates $x(t)$ to $y(t)$. The question of applicability is raised because $y^*(t)$ in this case may very well contain harmonic components with frequencies lower than ω . These components cannot be discarded on the basis of the filter hypothesis. The low-frequency components in $y^*(t)$ are due to higher harmonics of $y(t)$ which lie close to $l\omega_s$, and thus are modulated to frequencies near zero. Describing function theory would then seem to be applicable only if ω is so small that the effect of the sampling on the operation of the system is trivial.

2. If the frequency ratio ω/ω_s is rational, $\omega/\omega_s = m/n$, $y^*(t)$ is periodic with a frequency which is an integral multiple of ω/m . Again $y^*(t)$ may

contain harmonic components with lower frequencies than ω , and essentially the same comments about applicability of describing function theory made in regard to irrational frequencies are pertinent in this case.

3. If the frequency ratio ω/ω_s is a whole fraction, $\omega/\omega_s = 1/n$, $y^*(t)$ is periodic with frequency ω . It contains no harmonic component with frequency lower than ω , except possibly for a dc component, if $\omega < \frac{1}{2}\omega_s$. With the possible effects of a dc component taken into consideration, these are the right conditions for applicability of describing function theory, and the remainder of the chapter is restricted to this case. Fortunately, this includes a most important class of problems since the limit cycles which are most commonly observed in sampled nonlinear systems have periods which are whole multiples of the sampling period. It is important to observe that the component of frequency ω in $y^*(t)$ is not just $1/T_s$ times the corresponding component of $y(t)$. Thus it would be quite incorrect to employ a describing function which relates $x(t)$ to $y(t)$ and ignores the higher harmonics of a signal which is being sampled. *It is essential that the describing function characterize directly the relation between $x(t)$ and $y^*(t)$.*

As another illustration, consider the system configuration of Fig. 9.0-1b. In this case the higher harmonics in $y(t)$ are attenuated by the continuous linear filter before being sampled. Thus the modulating effect of the sampler on these harmonics may be of little importance. The greater question in this case is whether the input to the nonlinearity can be assumed a sinusoid. The hold does not provide very complete filtering of the high-frequency content of the sampled signal. Thus, unless there were additional filtering in the position of the hold, it might be necessary to characterize the transfer from $z(t)$ to $y(t)$ by a describing function—a task which promises to be laborious.

The following sections deal with the determination of and stability of limit cycle modes in sampled nonlinear systems, where the limit cycles tested have periods which are whole multiples of the sampling period. These are not the only limit cycles which may be possible in such systems but experience with both real and simulated systems has shown these to be by far the most commonly occurring modes. This does not exhaust the usefulness of describing function theory in its application to sampled nonlinear systems. But other applications, such as the study of forced sinusoidal response, must be considered carefully in each individual case because of the possibility of lower-frequency components, as discussed above under irrationally related frequencies, and the possible existence of limit cycle modes in addition to the forced response. A very important special-case system which can be dealt with by a simple extension of previous techniques is treated in the following section. Then, in the next, we turn to the study of limit cycles in more general systems.

9.1 LIMIT CYCLES IN SAMPLED TWO-LEVEL RELAY SYSTEMS

The material presented in Sec. 9.2 is readily applicable to the study of limit cycles in two-level relay systems, but these systems are of such importance that it seems worth exploiting the simpler approach which is possible in this case.

The configuration of the system is shown in Fig. 9.1-1. The two-level relay is shown as having possible hysteresis. A zero-order hold is considered to follow the sampling switch. A great many systems do employ a zero-order hold or simple clamp which clamps a sampled signal to a constant over the following sampling period. This analysis is not, however, limited to such systems. If the actual system does not include a hold, or uses a higher-order hold, the transfer function of that hold is included in the linear part, as shown in Fig. 9.1-1, along with the reciprocal of the zero-order-hold transfer function. The linear part may include any number of continuous and discrete linear elements.

THE DESCRIBING FUNCTION

One has free choice in deciding how much of the system to characterize with a describing function, so long as the nonlinear part is included. The analysis of this system is most like the analysis of continuous systems considered heretofore, if one chooses to represent the effect of the nonlinearity, the sampling switch, and the zero-order hold by a describing function. To this end, $x(t)$ is taken to be a sinusoid, unbiased to begin with, and the fundamental harmonic component of $z(t)$ is calculated. The frequencies we shall consider, according to the discussion of the preceding section, are whole fractions of the sampling frequency ω_s . Moreover, we shall center attention on the even fractions, $\frac{1}{2}$, $\frac{1}{4}$, $\frac{1}{6}$, . . . , since these are the limit cycle modes one might expect to see in the very common case in which the linear part of the system includes a pole at the origin, an integration. In that case $z(t)$ must be an unbiased function in any steady-state limit cycle with no input to the

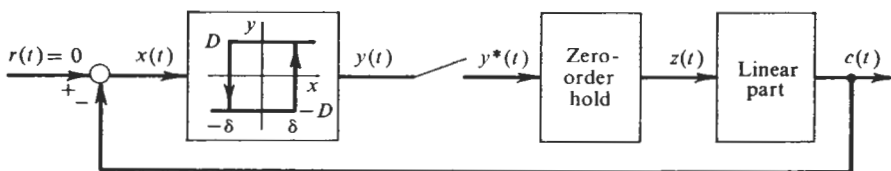


Figure 9.1-1 Two-level relay system configuration.

system. The drive signal into the linear part will then consist of a periodic cycle which includes an equal number of sampling periods of plus and minus drive. The only arrangement of these periods of plus and minus drive which is consistent with the sinusoid assumed as the input to the nonlinearity is n positive drive periods followed by n negative drive periods in the case of a cycle with period $2nT_s$, T_s being the sampling period. Such a cycle will be termed an n, n mode.

The input and output waveforms for the 2, 2 mode are shown in Fig. 9.1-2. $x(t)$ is a sinusoid with period $4T_s$, and $z(t)$ is a square wave with that period. The output of the hold, $z(t)$, is shown lagging the output of the nonlinearity, $y(t)$, because $y(t)$ is not in phase with the sampling points. The lag between the zero crossing of $y(t)$ and the next sampling point is not known a priori; evidently it can take any value between 0 and T_s in time or 0 and π/n in phase angle. The amplitude of the fundamental harmonic of $z(t)$ is $(4/\pi)D$, and the phase lag of that component relative to $x(t)$ is $\sin^{-1}(\delta/A) + \varphi$, where φ is the sampling lag. The describing function for the chain of elements—nonlinearity, sampling switch, and hold—is then

$$N(A, \varphi) = \frac{4D}{\pi A} \angle -\sin^{-1} \left(\frac{\delta}{A} \right) - \varphi \quad 0 < \varphi < \frac{\pi}{n}, A > \delta \quad (9.1-1)$$

This expression holds for an n, n mode of any order.

THE LINEAR PART

The remainder of the system, the linear part as shown in Fig. 9.1-1, is now characterized by its steady-state sinusoidal response at the frequency $(1/2n)\omega_s$.

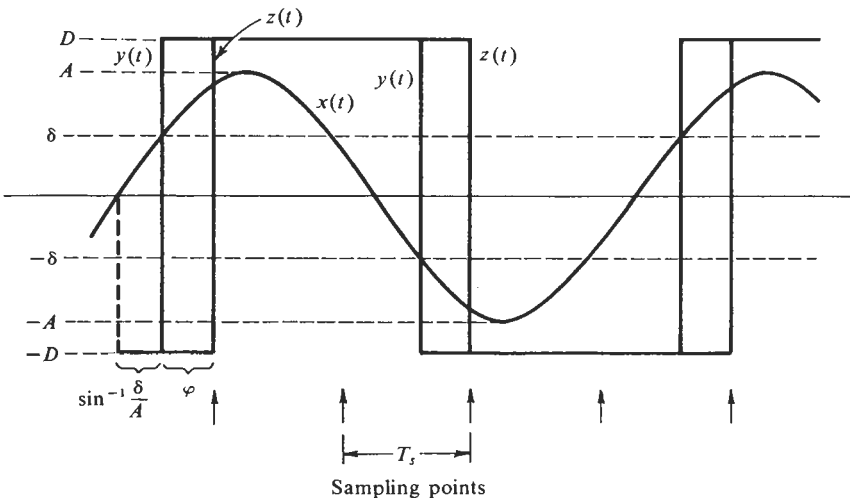


Figure 9.1-2 Signal waveforms for the 2, 2 mode.

If this is a continuous linear operator, the only requirement for applicability of describing function theory is that it attenuate the higher harmonics of $z(t)$ sufficiently to return essentially the fundamental sinusoid to $x(t)$. If this includes samplers and discrete linear elements, a more restrictive condition is placed on them. Consider the linear elements in Fig. 9.1-3. In this example, L_1 and L_2 represent continuous linear filters, whereas D represents a discrete linear filter. It may be mechanized as a pulsed analog filter, or perhaps as a digital computer solving a linear difference equation. L_1 and/or L_2 may include data holds. We wish to find the sinusoidal component of frequency ω in the steady-state output of this chain when the input is periodic with that frequency.

$$\begin{aligned} C(j\omega) &= L_2(j\omega)V^*(j\omega) \\ &= L_2(j\omega)D(j\omega)W^*(j\omega) \end{aligned} \quad (9.1-2)$$

But $W(j\omega) = L_1(j\omega)Z(j\omega)$

and $W^*(j\omega) = \frac{1}{T_s} \sum_{l=-\infty}^{\infty} L_1[j(\omega + l\omega_s)]Z[j(\omega + l\omega_s)]$

so $C(j\omega) = \frac{1}{T_s} L_2(j\omega)D(j\omega) \sum_{l=-\infty}^{\infty} L_1[j(\omega + l\omega_s)]Z[j(\omega + l\omega_s)]$ (9.1-3)

From this expression one can see that if $z(t)$ were just a sinusoid of frequency $\omega < \frac{1}{2}\omega_s$, none of the complementary components of $w^*(t)$ would have the frequency ω . The only component of $c(t)$ which would have the frequency ω is that due to the $l = 0$ term in the sum of Eq. (9.1-3). Thus the sinusoidal response function representing the fundamental transfer through the chain of elements in Fig. 9.1-3 would be just $(1/T_s)L_1(j\omega)D(j\omega)L_2(j\omega)$.

This result is complicated, however, by the fact that, in the system under study, $z(t)$ is a periodic function which includes harmonics in addition to the fundamental component. With ω an even fraction of ω_s , some of the odd harmonics of $z(t)$ are modulated to additional components of $w^*(t)$ at the frequency ω . The harmonics which contribute to the fundamental component after sampling are those with frequencies equal to $l\omega_s \pm \omega$, for all integers l . The effect of any significant contributors could be included by calculating the harmonics of $z(t)$, passing them through $L_1(jk\omega)$ (k is the order of the harmonic), and adding the term in Eq. (9.1-3). However, for

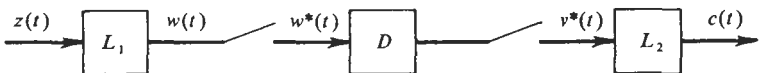


Figure 9.1-3 An example linear part.

simple application of the theory of this section, we must insist that the harmonic content of $z(t)$ be sufficiently attenuated before it reaches the first sampler in the linear part. An alternative procedure to treat this problem is discussed in the following section.

DETERMINATION OF MODES

Having a describing function $N(A, \varphi)$ to characterize the nonlinear part, sampler, and hold, and a steady-state sinusoidal response function $L(j\omega)$ to characterize the remaining linear part, the condition for the possible existence of a limit cycle mode is, as always,

$$1 + N(A, \varphi)L(j\omega) = 0 \quad (9.1-4)$$

The gain-phase plot is a convenient means of displaying the solutions to this equation. Although only the frequencies $(1/2n)\omega_s$ are of interest, it is often useful—especially for the later design of compensation—to plot the complete $L(j\omega)$ function. A typical curve is shown in Fig. 9.1-4. Solutions of Eq. (9.1-4) are represented by intersections of this curve of $L(j\omega)$ with $-1/N(A, \varphi)$. $N(A, \varphi)$, in this case, is defined only for the discrete set of frequencies $(1/2n)\omega_s$, and it depends both on A and n , the order of the mode. It is convenient to separate that part of N which depends only on A from that which depends on n for simplicity in plotting the function. Thus define

$$N'(A) = \frac{4D}{\pi A} \begin{array}{l} / \\ \hline \end{array} -\sin^{-1} \frac{\delta}{A} \quad (9.1-5)$$

which is the describing function given in Eq. (9.1-1), except for the sampling lag φ . This φ may take any value in the range $(0, \pi/n)$, and since this range depends on n —and thus ω —the bands of possible sampling lags can conveniently be shown as lines originating at the point of $L(j\omega)$ for each frequency and extending a distance corresponding to π/n . With the sampling lag accounted for separately in this manner, the describing function which is plotted, $-1/N'(A)$, is nothing more than the describing function for the two-level relay with hysteresis as it appears in continuous systems.

The completed plot (Fig. 9.1-4) indicates all possible limit cycle modes. For the typical case shown, the only intersections of $L(j\omega)$ plus the sampling lag with $-1/N'(A)$ occur at the frequencies $\frac{1}{8}\omega_s$ and $\frac{1}{4}\omega_s$. Thus only the 3, 3 and 4, 4 modes are possible in this case. The higher-frequency modes are not possible because the nonlinearity and linear part have too much phase lag even if the sampling action contributes none, and the lower-frequency modes are not possible because even with the maximum possible sampling delay, the sinusoidal signal does not accumulate 360° of phase lag around the loop. The intersections indicating the possible modes are encircled in the figure. The frequency of each mode is indicated on the scale of $L(j\omega)$ at that

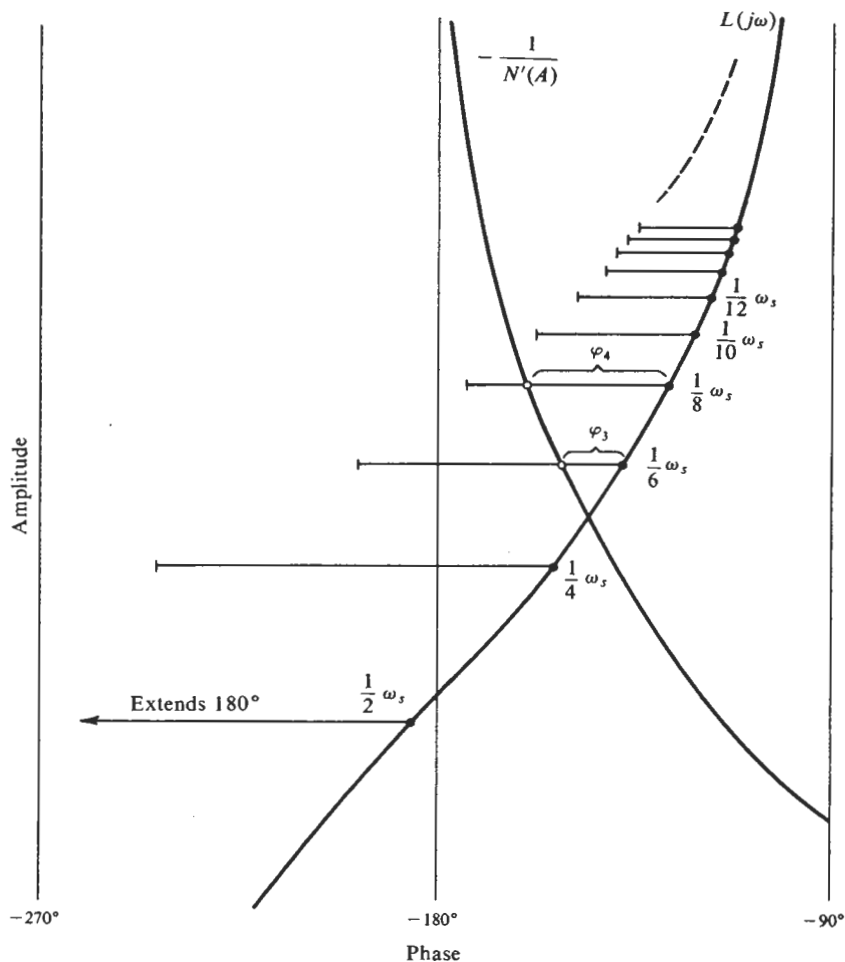


Figure 9.1-4 Gain-phase plot for sampled two-level relay system.

point; the amplitude of each mode at the input to the nonlinearity is indicated on the scale of $-1/N'(A)$ at that point; and the phase lag due to the sampling delay in each mode is indicated by the phase difference between $L(j\omega)$ and $-1/N'(A)$ at those points.

Notice that for frequencies much smaller than the sampling frequency, the possible limit cycle frequencies become closely spaced and the maximum sampling lag is small. In this low-frequency region the sampling has little effect on the behavior of the system.

When more than one limit cycle mode is possible, the limit cycle which will be observed depends on the prior history of the system variables. If the modes are stable (this matter is discussed in a later section), there is some

region of initial conditions from which the system will settle into each mode. These regions are often much smaller for some modes than for others, and so some modes are more likely to occur than others. In any case, a system must be designed so that all possible modes are acceptable. If one or more indicated modes are not acceptable, usually because the amplitude at some point in the system is too large, these modes must be eliminated by compensation.

DESIGN OF COMPENSATION

It is at this point in the design of systems that one of the great advantages of the use of describing functions becomes apparent. In most instances the compensation required to improve those performance characteristics which can be evaluated by the use of describing functions is quite evident. So it is in this instance. If the 4, 4 mode as indicated on Fig. 9.1-4 has an unacceptably large amplitude, it can be eliminated by providing at least $(45 - \varphi_4)$ deg of phase lead at the frequency $\frac{1}{8}\omega_s$, somewhere around the loop. After such compensation, the 3, 3 mode will still be possible, and in all likelihood one or both of the higher-frequency modes as well. If the 3, 3 mode is to be eliminated also, the compensation is designed to provide at least $(45 - \varphi_4)$ deg of lead at $\frac{1}{8}\omega_s$, and at least $(60 - \varphi_3)$ deg of lead at $\frac{1}{6}\omega_s$. The amplitudes of the remaining possible modes at various stations around the loop will differ with the location of the compensation, and this can be evaluated using just steady-state frequency response characteristics.

This linear compensation can be implemented with either a continuous or discrete compensator. Alternatively, the design problem might be to find that value of hysteresis, δ , in the switching characteristic which will allow only modes up to order n , for some specified value of n . In this case, too, the answer to the problem is fairly evident, using describing function theory. For the case pictured in Fig. 9.1-4, the 4, 4 mode can be eliminated by reducing δ , but other modes would remain possible since, in the limit as $\delta \rightarrow 0$, the curve of $-1/N'(A)$ extends along the entire phase = -180° line.

BIAS OFFSET

In the foregoing discussion, the limit cycle modes have been considered unbiased sinusoids. The fact that some systems may sustain a dc offset around part of the loop is another important difference between sampled and continuous systems. If the linear part of the system does not include an integrator, a steady-state bias signal could exist only if such a signal could regenerate itself when propagated around the loop. But this will not be possible with this nonlinearity and ordinary linear parts because a positive bias in $x(t)$ (refer to Fig. 9.1-1) will cause a positive bias, if any, in $z(t)$, and

this will be transferred through the linear part to a positive bias in $c(t)$. But this is inconsistent with the assumed positive bias in $x(t)$. Thus, if the system is stable to the low-frequency signal in the presence of the limit cycle, the bias will decay to zero at all stations around the loop.

If the linear part includes an integrator, the input to it, $z(t)$ in Fig. 9.1-1, must be unbiased in any steady-state mode with no input to the system. This does not, however, preclude a bias in $c(t)$ and $x(t)$. Any bias in these signals is possible so long as the output of the nonlinearity remains unbiased. The range of possible bias offsets can be seen in Fig. 9.1-5, where the signal waveforms through the nonlinearity and hold have been drawn for the 3, 3 mode of the system of Fig. 9.1-4, and the proper sampling lag, φ_3 , taken from that figure, is shown. The points in time at which the samples are taken are shown as dots on the $x(t)$ waveform. It is clear that the $x(t)$ curve could be shifted up or down by a small bias without changing the output $z(t)$ at all. The range of this possible offset, to which the system is insensitive, is determined by noting how far $x(t)$ can be shifted without changing $y(t)$ (see Fig. 9.1-1) at the sampling points. For the case shown in Fig. 9.1-5, it is the sampling points at which $z(t)$ switches which are critical, and the range of possible bias offset is indicated. In other cases, it may be one of the other sampled points which first causes a change in $z(t)$. The bias range shown in the figure is that of $x(t)$, the input to the nonlinearity. This range can be reflected to other signals in the linear part of the system, using the dc gain of the system between the two points. The signals between $z(t)$ and the integrator in the linear part remain unbiased.

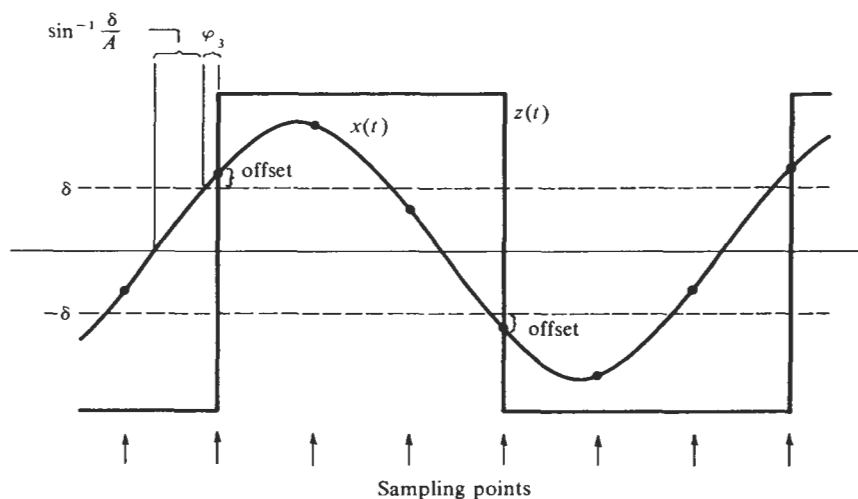


Figure 9.1-5 Nonlinearity input and output showing range of possible bias offset.

Compensation designed to improve limit cycle moding will affect the range of bias offset as well, sometimes adversely. In some systems, the possibility of a dc error which the system does not respond to is of greater consequence than the possible limit cycle modes. If the bias range is unacceptably large, compensation must be designed to reduce it. This is done by introducing (if possible) a larger dc gain relative to the limit cycle gain between the error point and the input to the nonlinearity. This can be achieved by a conventional lag-lead compensator which has high gain at low frequencies and unity gain with negligible phase lag at the limit cycle frequencies. An integrator with a bypass can eliminate the dc offset at the error point altogether.

9.2 LIMIT CYCLES IN OTHER SAMPLED NONLINEAR SYSTEMS

From the experience of the preceding section we observe some of the important characteristics of a describing function analysis of sampled nonlinear systems. The describing function was found to depend not only on the amplitude of the sinusoid assumed at the input to the nonlinearity, but also on the ratio of the sinusoidal frequency to the sampling frequency and the phase of the sampling points relative to the input sinusoid. The frequency-ratio and phase-angle dependencies were also found in the two-sinusoid-input describing function for continuous systems in the case of rationally related frequencies. The present situation is somewhat analogous to that: again, there are two periodic processes operative in the system, and their periods are rationally related. Instead of two periodic signals, however, the periodic processes in this case are one sinusoidal signal and the periodic sampling process.

Analysis of limit cycles in sampled two-level relay systems was found to be not much more difficult than the corresponding analysis of continuous two-level relay systems. This is due to the simple way in which the frequency-ratio and phase-angle dependencies enter that problem. The nonlinearity output in that case is known to be a square wave if it is nontrivial. Thus the fundamental amplitude of the output is independent of the frequency ratio or phase angle. The sampling phase simply adds directly to the phase angle of the describing function, and the frequency ratio plays no role other than to prescribe the bound on possible sampling lag.

For other nonlinearities, the basic concepts remain unchanged, but the details are more complicated because the whole waveform of the nonlinearity output changes with sampling phase angle. This complicates considerably the calculation of the describing function for a sampled nonlinearity for all input amplitudes, frequency ratios, and phase angles relative to the sampling points. However, once the computation is done and the

results graphed, the use of the describing function to analyze system limit cycles and to design compensation to meet specifications on possible limit cycle modes is just as easy and meaningful as it is for continuous systems.

TWO POINTS OF VIEW

The general system configuration under consideration is shown in Fig. 9.2-1. The configuration is characterized by a single loop with a single separable nonlinear part. The linear parts L_1 , L_2 , and L_3 provide continuous linear filtering, and may include samplers and discrete linear elements as well. The major requirement for applicability of describing function theory is that the signal which is assumed sinusoidal, $x(t)$ in this case, must indeed approximate that waveform. This means, in the case of sampled systems, that not only the harmonic content of the nonlinearity output, but also the harmonic content due to all samplers in the system, must be adequately attenuated in the linear filter which returns the signal to the nonlinearity input.

In addition to any samplers which may be included in the linear parts, one is shown specifically following the nonlinearity. It is a sampler such as this, operating directly at the input or output of a nonlinearity, which gives rise to the greatest difference between continuous- and sampled-nonlinear-system operation. For the system as shown, it would be a very poor approximation to use an ordinary describing function to characterize the transfer from $x(t)$ to $y(t)$, and characterize the rest of the system by its steady-state sinusoidal response at the fundamental frequency. The major error in that approach would be the neglect of the higher harmonics of $y(t)$ in determining the fundamental component of $y^*(t)$. The sampling operation modulates some of the higher harmonics of $y(t)$ down to fundamental-frequency components of $y^*(t)$. Thus any reasonable describing function approach must model directly the transfer from $x(t)$ to $y^*(t)$. A similar situation would hold if the sampler preceded the nonlinearity, as shown in Fig. 9.2-2a. In that case, the hold does not filter the harmonics because of the sampling operation sufficiently to justify the assumption of a sinusoid at $y(t)$, the input to the nonlinearity. Thus the describing function must be defined to characterize

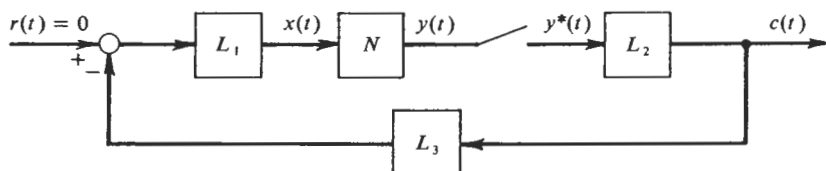


Figure 9.2-1 The general sampled-nonlinear-system configuration considered in this section. L_1 , L_2 , L_3 may include additional samplers and both continuous and discrete linear elements.

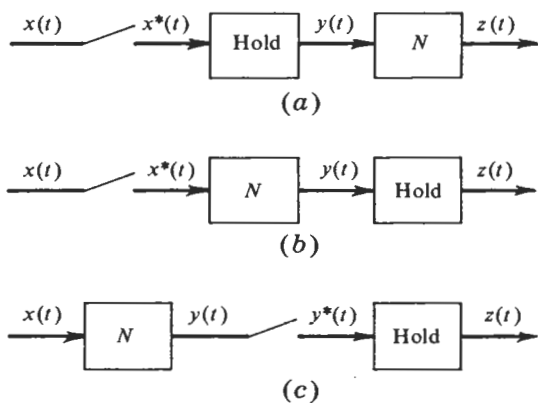


Figure 9.2-2 Equivalent arrangements for static, single-valued nonlinearities.

directly the transfer from $x(t)$ to $z(t)$. If the nonlinearity is static and single-valued so that the output depends only on the current value of the input, the three orderings of sampler, hold, and nonlinearity shown in Fig. 9.2-2 are equivalent. This implies that in arrangement *b* the nonlinear operation is carried out on the impulses at the input to yield impulses at the output whose areas or strengths are related to those at the input by the given nonlinear function. If the nonlinearity were dynamic or multiple-valued, the order of the arrangement would matter, and the describing function would have to be calculated for the given arrangement. For the present we shall refer to arrangement *c*, and include the hold in the linear part of the system. This is the arrangement shown in Fig. 9.2-1.

Two different approaches to the describing function analysis of systems such as that of Fig. 9.2-1 have been set forth. One is the same approach taken in the preceding section as applied to two-level relay systems. Chow (Ref. 2) documented this point of view, which was being developed by Russell (Ref. 23) at the same time. They defined a describing function for a nonlinearity, sampler, and zero-order hold in the classical way—the amplitude and phase relation between an assumed sinusoid at the input and the fundamental component of the periodic output. The use of the hold in the chain of elements for which the describing function was defined is not essential to this approach. Referring again to Fig. 9.2-1, one can better calculate a describing function to characterize just the transfer from $x(t)$ to $y^*(t)$ using the same point of view—representation of the fundamental harmonic response of the nonlinearity and sampler. This has the advantage of greater generality since it is applicable to the sampled nonlinearity regardless of what kind of hold, if any, is used in the system. If a hold does indeed follow the sampler, it is then included in the linear part of the system. As a lesser advantage, it may be noted that the calculation of the fundamental

component of $y^*(t)$ is particularly simple since that function is just a sequence of impulses. The describing function which relates an assumed sinusoid at the input to a nonlinearity to the fundamental component of the sampled output of the nonlinearity will here be termed a *sampled describing function*.

$$N(A, \varphi) = \text{sampled describing function} \\ = \frac{\text{phasor representation of fundamental component of } y^*(t)}{\text{phasor representation of } x(t)}$$

With the transfer from $x(t)$ to the fundamental component of $y^*(t)$ in Fig. 9.2-1 given by the sampled describing function, the linear part of the system is characterized by its steady-state sinusoidal response at the fundamental frequency.

Another approach to this problem was documented by Kuo (Refs. 14, 15). With the input to the nonlinearity, $x(t)$, assumed to be a sinusoid of a frequency which is a whole fraction of the sampling frequency, the sampled output of the nonlinearity, $y^*(t)$, is a periodic sequence of impulses with the same period as the input. The z transform of the output sequence can be written explicitly, and the ratio of that z transform to the z transform of the input sinusoid is defined by Kuo to be the *z-transform describing function* for the nonlinearity and sampler.

$$N^*(A, \varphi) = \text{z-transform describing function} \\ = \left[\frac{\text{z transform of } y^*(t)}{\text{z transform of } x(t)} \right]_{\text{Fundamental frequency}}$$

With the relation between samples of $x(t)$ to samples of $y(t)$ defined by the z -transform describing function, the linear part of the system is characterized by its sampled transfer function, and the equation of loop closure which defines a possible limit cycle mode is evaluated at the fundamental frequency.

These two points of view are basically different. The difference in results using the two approaches is trivial in some instances and quite significant in others. If one approach were superior on all counts, the other could be discarded at once. But this is not the case; so the control engineer should keep both techniques in his bag of analytic tools and understand when to use each one. The major advantage of the first approach, the sampled describing function, is its simplicity. The analytic manipulations involved, for example, in determining the range of system parameters for which a particular limit cycle mode is possible, are considerably simpler using the sampled describing function approach. This advantage in simplicity is due to the use of the ordinary sinusoidal response function for the linear part, rather than the sampled transfer function. For this same reason, the design of compensation to meet specifications on limit cycle modes is obvious when the sinusoidal

response function is used, but obscure when a new sampled transfer function must be calculated for the cascaded compensation and original linear part. The major advantage of the second approach, the z -transform describing function, is its better accuracy in some situations. Using this technique, the exact pulse sequence at the nonlinearity output is processed exactly through the linear part using z transforms. This can be done without approximation for any linear configuration of continuous elements, samplers, and discrete elements. The result is the z transform of the signal fed back to the nonlinearity input. This transform contains terms which define the fundamental frequency component of the fed-back samples, ripple terms, and the normal modes of the linear part of the system. This function is clearly not compatible with the simple sinusoid originally assumed at the nonlinearity input. But the process of equating the transform of the fed-back function to the transform of the originally assumed sinusoid *when both are evaluated at the fundamental frequency* serves to select just the fundamental component of the fed-back samples and equate it to the assumed sinusoid. Thus the sequence of samples of the fed-back signal is being accurately determined in this case, and it is the fundamental harmonic component of this exact pulse train which is being equated to the sinusoid originally assumed at the nonlinearity input.

By contrast, using the sampled describing function approach, the harmonics of $y^*(t)$ are dropped immediately, and only the fundamental component is passed through the linear part. If the linear part contains no additional samplers, the fundamental component of the signal fed back to the nonlinearity input is correctly determined by this procedure, and the only difference between the two techniques is the difference between the fundamental component of the continuous signal fed back to the nonlinearity and the fundamental component of the samples of that signal. Since the fundamental component of the samples of a sinusoid, for $\omega_s > 2\omega$, is just $1/T_s$ times the sinusoid itself, it can be seen that the two techniques must give very nearly the same results if the assumption which is common to both is well satisfied, namely, that the signal fed back to the nonlinearity closely approximates a sinusoid. In that case, the sampled describing function is to be preferred because of its simplicity. If the linear part fails to filter the fed-back signal well enough, the fundamental component of the samples of the fed-back signal may differ from the fundamental component of the continuous fed-back signal, and in that case the z -transform describing function is likely to give the more nearly correct answer because it recognizes the fed-back signal only at the sampling instants, as does the nonlinearity. The fundamental component of the continuous fed-back signal, on the other hand, is influenced by the shape of the signal between the sampling points; and this is of no consequence to the nonlinearity. In this case of inadequate filtering, however, the use of describing function theory by either method is risky.

When the linear part contains additional samplers and discrete linear elements, the case for the z -transform describing function is stronger. As noted above, the samples of the fed-back signal can be determined exactly, no matter what the configuration of the linear part. Dropping the higher harmonics of $y^*(t)$, as is done when using the sampled describing function, can be serious in this case because a sampler in the linear part will modulate some of these harmonics down to additional contributions to the fundamental frequency component. Thus, with additional samplers in the linear part, propagation of only the fundamental component of $y^*(t)$ through the sinusoidal response function for the linear part does not correctly determine the fundamental component of the fed-back signal at the nonlinearity input. The approximation will be good if the harmonics of $y^*(t)$ are well filtered before the signal encounters a sampler, but this is a requirement which need not be met for successful use of the z -transform describing function.

A basic limitation of the z -transform describing function should also be noted. Using that technique, one only processes information about the samples of the signals circulating in the system. Sinusoidal signals are defined by their samples in the sense that the fundamental component of the sampled sinusoid is a constant times the sinusoid itself only if the sampling frequency is greater than twice the frequency of the sinusoid. This means that the very important case of limit cycle modes which have a frequency just $\frac{1}{2}$ the sampling frequency cannot be analyzed by the z -transform describing function method.

Implementation of these two points of view will be clarified by an example analyzed by both methods.

Example 9.2-1 The system of Fig. 9.2-3 uses an ideal two-level relay as a controller. It drives a digital integrator which implements the rectangular-rule integration formula

$$v(kT_s) = v[(k-1)T_s] + y[(k-1)T_s]T_s, \quad (9.2-1)$$

which has the z transform

$$V^*(z) = z^{-1}V^*(z) + z^{-1}Y^*(z)T_s$$

or

$$D^*(z) = \frac{V^*(z)}{Y^*(z)} = \frac{T_s}{z-1} \quad (9.2-2)$$

The output of the integrator is held constant between sampling instants, and the held signal feeds back through a continuous linear filter, which we take to be

$$L(s) = \frac{K}{\tau s + 1} \quad (9.2-3)$$

This example is deliberately chosen to have poor filtering of the fed-back signal so that the difference between the two describing function methods will be dramatized.

Determine the conditions under which the 2, 2 limit cycle mode is possible in this system.

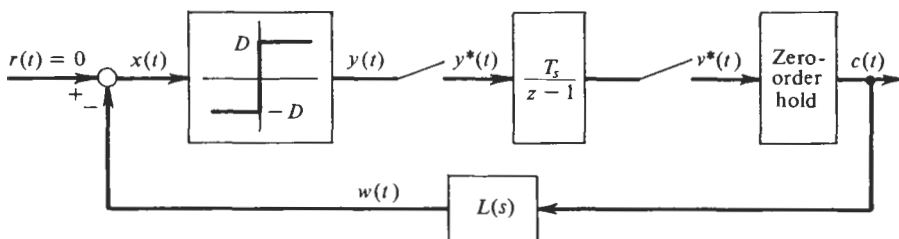


Fig. 9.2-3 System configuration for Example 9.2-1.

First solution The phase relation between the sinusoid assumed at $x(t)$ and the sampling points may vary between 0 and T_s in time or 0 and $\pi/2$ radians in angle. Take the time origin to coincide with one of the sampling points. Then, with respect to this origin, $x(t)$ is advanced in phase by an angle which may range between 0 and 90° .

$$x(t) = A \sin \left(\frac{\omega_s}{4} t + \varphi \right) \quad 0 < \varphi < 90^\circ \quad (9.2-4)$$

$y(t)$ is then a square wave with amplitude $\pm D$, and $y^*(t)$ a periodic sequence of impulses with strengths $\pm D$, as shown in Fig. 9.2-4. The fundamental component of $y^*(t)$, shown dashed in that figure, is obviously advanced in phase by 45° with respect to the time origin, and its amplitude can be computed directly as the amplitude of the fundamental frequency sine component having that phase angle.

$$\begin{aligned} |y_r^*(t)| &= \frac{2}{2T_s} \int_{0-}^{2T_s-} y^*(t) \sin \left(\frac{\omega_s}{4} t + 45^\circ \right) dt \\ &= \frac{1}{T_s} (D \sin 45^\circ + D \sin 135^\circ) \\ &= \sqrt{2} \frac{D}{T_s} \end{aligned} \quad (9.2-5)$$

In the calculation of the fundamental component of a signal which consists of or includes impulse functions, impulses should not be included at both end points of the interval of integration. The integration can include the impulse at either end point, but not both. From Eqs. (9.2-4) and (9.2-5), the sampled describing function for the ideal two-level relay in the case of the 2, 2 mode is seen to be

$$N(A, \varphi) = \frac{\sqrt{2}}{T_s} \frac{D}{A} \angle 45^\circ - \varphi \quad 0 < \varphi < 90^\circ \quad (9.2-6)$$

The sinusoidal response function for the linear part of this system is determined by the following calculation:

$$\begin{aligned} W(j\omega) &= L(j\omega)H(j\omega)V^*(j\omega) \\ &= L(j\omega)H(j\omega)D^*(j\omega)Y^*(j\omega) \end{aligned} \quad (9.2-7)$$

where $H(j\omega)$ is the sinusoidal response function for the zero-order hold. For this linear part, the fundamental component of $w(t)$ is correctly given by the fundamental component of $y^*(t)$, modified by the sinusoidal response function $D^*(j\omega)H(j\omega)L(j\omega)$, evaluated at the

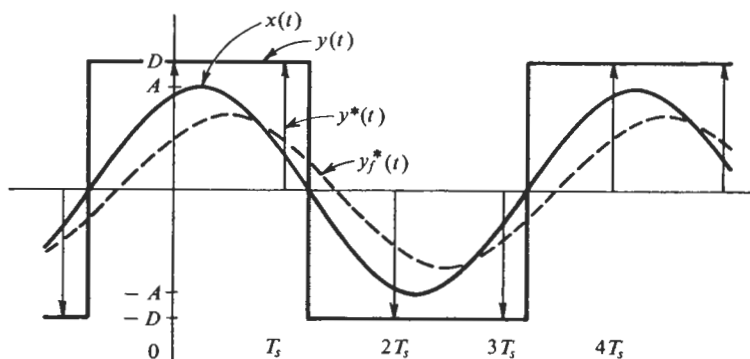


Figure 9.2-4 Nonlinearity input and output for Example 9.2-1.

frequency $\omega = \omega_s/4$. If the nonlinearity and sampler were followed by a continuous linear element, and then a sampler and discrete linear element, this would not be true. In evaluating $D^*(z)$ at $\omega = \omega_s/4$, we note $z = e^{sT_s} \rightarrow e^{j(1/4)\omega_s T_s} = j$. Also, the zero-order hold has the sinusoidal response function

$$H(j\omega) = \frac{1 - e^{-j\omega T_s}}{j\omega} \quad (9.2-8)$$

so

$$D^*HL\left(j\frac{\omega_s}{4}\right) = \frac{T_s}{j-1} \frac{1+j}{j\frac{\pi}{2}\frac{1}{T_s}} \frac{K \left\langle -\tan^{-1} \frac{\pi}{2} \frac{\tau}{T_s} \right\rangle}{\sqrt{1 + \left(\frac{\pi}{2} \frac{\tau}{T_s}\right)^2}}$$

$$= \frac{2}{\pi} T_s^2 \frac{K}{\sqrt{1 + \left(\frac{\pi}{2} \frac{\tau}{T_s}\right)^2}} \left\langle -180^\circ - \tan^{-1} \frac{\pi}{2} \frac{\tau}{T_s} \right\rangle \quad (9.2-9)$$

Equating the fundamental component of $w(t)$ to $-x(t)$ requires

$$ND^*HL = -1$$

or

$$\frac{2\sqrt{2} KDT_s}{\pi A} \frac{1}{\sqrt{1 + \left(\frac{\pi}{2} \frac{\tau}{T_s}\right)^2}} \left\langle 45^\circ - 180^\circ - \varphi - \tan^{-1} \frac{\pi}{2} \frac{\tau}{T_s} \right\rangle = 1 \left\langle -180^\circ \right\rangle$$

Solving for A and φ , we find

$$A = \frac{2\sqrt{2}}{\pi} \frac{KDT_s}{\sqrt{1 + \left(\frac{\pi}{2} \frac{\tau}{T_s}\right)^2}} \quad (9.2-10)$$

$$\varphi = 45^\circ - \tan^{-1} \frac{\pi}{2} \frac{\tau}{T_s} \quad (9.2-11)$$

Since φ must lie in the range $(0, 90^\circ)$, Eq. (9.2-11) can be satisfied for all values of τ/T_s in the range

$$-\frac{2}{\pi} < \frac{\tau}{T_s} < \frac{2}{\pi}$$

It will later be determined that the indicated limit cycle mode is stable only if the open-loop system is stable. Thus one would conclude from application of sampled describing function theory that the 2, 2 limit cycle mode may exist if $(0 < \tau/T_s < 2/\pi)$.

Second solution For application of z-transform describing function theory to this problem we first write the z transform of $x(t)$.

$$x(t) = A \cos \varphi \sin \frac{\omega_s}{4} t + A \sin \varphi \cos \frac{\omega_s}{4} t \quad (9.2-12)$$

Use of a standard table of z transforms gives

$$X^*(z) = \frac{Az}{z^2 + 1} (\cos \varphi + z \sin \varphi) \quad (9.2-13)$$

The sampled output of the nonlinearity is seen in Fig. 9.2-4 to have the transform

$$\begin{aligned} Y^*(z) &= D + Dz^{-1} - Dz^{-2} - Dz^{-3} + Dz^{-4} + \dots \\ &= \frac{1 + z^{-1}}{1 + z^{-2}} D \\ &= \frac{z(z + 1)}{z^2 + 1} D \end{aligned} \quad (9.2-14)$$

The z-transform describing function is then

$$\begin{aligned} N^*(A, \varphi) &= \frac{Y^*(z)}{X^*(z)} \\ &= \frac{D}{A} \frac{z + 1}{\cos \varphi + z \sin \varphi} \end{aligned} \quad (9.2-15)$$

The sampled transfer function for the linear part of the system is calculated by standard procedures, again referring to a table of z transforms.

$$\begin{aligned} (D^*HL)^* &= \left(\frac{T_s}{z-1} \frac{z-1}{zs} \frac{K}{\tau s + 1} \right)^* \\ &= \frac{T_s}{z} \left[\frac{K}{s(\tau s + 1)} \right]^* \\ &= \frac{KT_s(1-a)}{(z-1)(z-a)} \end{aligned} \quad (9.2-16)$$

where

$$a = e^{-T_s/\tau} \quad (9.2-17)$$

Equating the fundamental component of the fed-back samples to $-x(t)$ requires

$$N^*(D^*HL)^*|_{\omega=\omega_s/4} = -1 \quad (9.2-18)$$

$$\frac{D}{A} \frac{j+1}{\cos \varphi + j \sin \varphi} \frac{KT_s(1-a)}{(j-1)(j-a)} = 1 \angle -180^\circ$$

Solving for A and φ yields, after some manipulation,

$$A = KDT_s \frac{1-a}{\sqrt{1+a^2}} \quad (9.2-19)$$

$$\varphi = -\tan^{-1} a \quad (9.2-20)$$

with a given by Eq. (9.2-17). Again, φ must lie in the range $(0, 90^\circ)$, but according to Eq. (9.2-20), it takes only negative values. Thus application of z -transform describing function theory leads to the conclusion that the 2, 2 limit cycle mode cannot be sustained by this system—a conclusion quite different from that reached using the sampled describing function previously.

Discussion Consideration of the shapes of the signals that would result in the linear part of this system for the given nonlinearity output readily confirms the conclusion reached by z -transform describing function analysis as correct. If the periodic pulse sequence $y^*(t)$ as shown in Fig. 9.2-4 were impressed on the linear part of this system, the steady-state response at $c(t)$ and $w(t)$ is shown in Fig. 9.2-5. It is clear that at $t = 0$, $w(t)$ must be greater than zero, and thus $x(t)$ must be less than zero. But this is inconsistent with a positive impulse in $y^*(t)$ at $t = 0$; so the mode is impossible. The failure of the sampled describing function method in this case is due to a rather slight difference in phase between the fundamental component of $w(t)$ and the fundamental component of $w^*(t)$. The fundamental component of $w(t)$, for small enough values of τ/T_s , crosses zero to the left of $t = 0$ and indicates that the mode is possible. But the fundamental component of $w^*(t)$ crosses zero to the right of $t = 0$ for all values of τ/T_s , and correctly indicates that the mode is impossible. The fed-back signal in this case, especially for small values of τ/T_s , does not approximate a sinusoid at all well, and one would expect possible difficulty in the use of describing function theory.

As noted before, this example, using only first-order continuous linear filtering, was deliberately chosen to emphasize possible differences in results using the two describing function points of view. In cases where the signal returned to the nonlinearity is better filtered, and where there is no problem with sampling of harmonically distorted signals in the system linear part, the two procedures yield very similar results, both of which are in close agreement with exact results. As an indication of this, consider another example in which second-order continuous linear filtering exists.

Example 9.2-2 The system of Fig. 9.2-6 uses an ideal two-level relay controller and first-order digital lead compensation. The remainder of the linear part consists of a zero-order hold and a continuous linear part

$$L(s) = \frac{K}{s(\tau s + 1)} \quad \tau = T_s \quad (9.2-21)$$

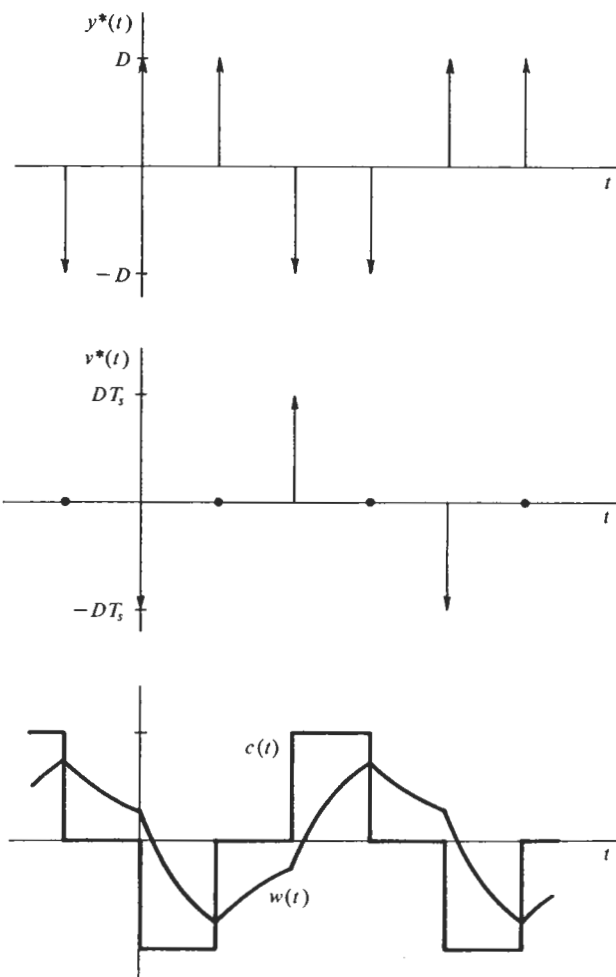


Figure 9.2-5 Signal waveforms in Example 9.2-1.

Determine the amount of lead (the value of a) necessary to render the 3, 3 limit cycle mode impossible.

Using procedures identical with those of the preceding example, we find

$$x(t) = A \sin \left(\frac{\omega_s}{6} t + \varphi \right) \quad 0 < \varphi < 60^\circ \quad (9.2-22)$$

Using the sampled describing function approach,

$$N(A, \varphi) = \frac{4D}{3AT_s} \underline{\underline{\quad / 30^\circ - \varphi \quad}} \quad 0 < \varphi < 60^\circ \quad (9.2-23)$$

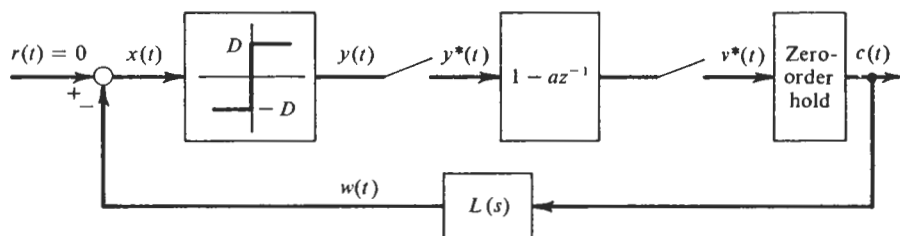


Figure 9.2-6 System configuration for Example 9.2-2.

and

$$D^*HL\left(j\frac{\omega_s}{6}\right) = \frac{K(1 - ae^{-j\pi/3})(1 - e^{-j\pi/3})}{-\left(\frac{\pi}{3}\frac{1}{T_s}\right)^2\left(1 + j\frac{\pi}{3}\frac{\tau}{T_s}\right)} \quad (9.2-24)$$

The solution of

$$ND^*HL = -1$$

gives

$$A = 0.839KDT_s \sqrt{(1 - 0.5a)^2 + (0.866a)^2} \quad (9.2-25)$$

$$\varphi = 43.7^\circ + \tan^{-1} \frac{0.866a}{1 - 0.5a} \quad (9.2-26)$$

The requirement that φ lie in the interval $(0, 60^\circ)$ dictates that the range of a for which the 3, 3 limit cycle mode is possible is

$$-2.46 < a < 0.289$$

Values of a outside this range render the mode impossible.

With the z -transform describing function approach we find

$$N^*(A, \varphi) = \frac{D}{A} \frac{z^2 + z + 1}{(z + 1)[0.866 \cos \varphi + (z - 0.5) \sin \varphi]} \quad 0 < \varphi < 60^\circ \quad (9.2-27)$$

and

$$(D^*HL)^* = KT_s \frac{(0.368z + 0.264)(z - a)}{z(z - 1)(z - 0.368)} \quad (9.2-28)$$

The solution of

$$N^*(D^*HL)^*|_{\omega=\omega_s/6} = -1$$

gives

$$A = 0.836KDT_s \sqrt{(0.5 - a)^2 + (0.866)^2} \quad (9.2-29)$$

$$\varphi = -15.9^\circ + \tan^{-1} \frac{0.866}{0.5 - a} \quad (9.2-30)$$

The requirement that φ lie in the interval $(0, 60^\circ)$ indicates in this instance that the range of a for which the 3, 3 limit cycle mode is possible is

$$-2.54 < a < 0.283$$

The calculated end points for this interval of a differ no more than 3 percent from those calculated by the sampled describing function technique. Also, in the two expressions for

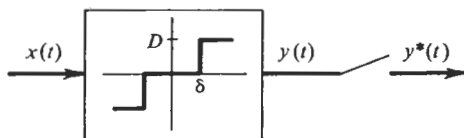
the amplitude of the limit cycle, Eqs. (9.2-25) and (9.2-29), the two radicals involving a are identical; so the expressions are seen to differ by just 0.4 percent.

Having discussed and illustrated these two points of view regarding describing function analysis of limit cycles in sampled nonlinear systems, we proceed to consider the calculation of these describing functions for nonlinearities other than the two-level relay, which has already been treated. An important observation should be made at the outset. In the preceding discussion, the point of view taken was that the samples of the nonlinearity output, or their fundamental component, are processed around the loop, and the fundamental component of the signal returned to the nonlinearity input is equated to the sinusoid originally assumed. When the z -transform describing function is calculated in advance and graphed for convenient use, the ratio of Y^* to X^* is immediately evaluated at the fundamental frequency. But the evaluation of Y^* at the fundamental frequency serves to select just the fundamental component from the $y^*(t)$ waveform. Also, evaluation of X^* at the fundamental frequency selects the fundamental component of $x^*(t)$. Since $x(t)$ is taken to be a sinusoid, the fundamental component of $x^*(t)$ is just $1/T_s$ times $x(t)$ for $T > 2T_s$. Thus, for $T > 2T_s$, the z -transform describing function is exactly T_s times the sampled describing function which relates the amplitude and phase of the fundamental component of $y^*(t)$ to $x(t)$. As noted before, for $T = 2T_s$ the z -transform describing function is not applicable; the sampled describing function is. Since in other cases the two describing functions are related by a known constant, only one calculation need be made. The easier calculation by far is that of the sampled describing function. The difference between the two points of view is then finally evidenced in the difference between the continuous and sampled transfer functions for the linear part of the system.

THE THREE-LEVEL RELAY

After the two-level relay, the nonlinearity of greatest importance in limit cycle analysis of sampled nonlinear systems is almost surely the three-level relay. In many instances in which a fixed drive level is desired, a zero level is included for the specific purpose of avoiding limit cycles in the absence of input. The nonlinearity under consideration is shown in Fig. 9.2-7. Calculation of the sampled describing function for this nonlinearity is in principle no different from the corresponding calculation for the two-level relay, but in practice is much more tedious because of the change in form of the output at the input level δ . This gives rise to a variety of different output mode shapes at every frequency, these modes depending on the amplitude and phase of the input. For most nonlinearities other than the two-level relay, the phase of the input sinusoid relative to the sampling points enters

Figure 9.2-7 The sampled three-level relay.



the problem in a more complicated way in that it affects the shape of the output waveform. The labor involved in describing function calculation is due to the necessity of enumerating all possible mode shapes and dealing with each one.

As an illustration of the calculation in the present case of the three-level relay, consider the possible modes of period $6T_s$. With the input assumed to be an unbiased sinusoid,

$$x(t) = A \sin(\omega t + \varphi) \quad (9.2-31)$$

With $\omega = \frac{1}{6}\omega_s = \pi/3T_s$,

$$x(t + 3T_s) = -x(t) \quad (9.2-32)$$

so the values of $y(t)$ at the first three sampling points determine $y(t)$ at all other sampling points. The sampling lag can range between zero and one sampling period, or

$$0 < \varphi < 60^\circ$$

in this case. The nonlinearity input at the times of the first three samples is then

$$x(0) = A \sin \varphi \quad (9.2-33)$$

$$x(T_s) = A \sin(60^\circ + \varphi) \quad (9.2-34)$$

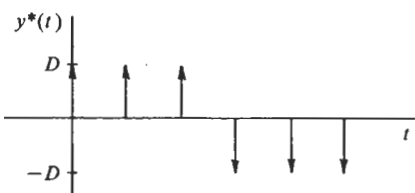
$$x(2T_s) = A \sin(120^\circ + \varphi) \quad (9.2-35)$$

In view of the limited range of φ , it is clear that $y(t)$ at these three sampling points can only be 0 or $+D$. This gives eight possible combinations of values, including the trivial zero output. But not all eight combinations are consistent with the sinusoidal form of the input. Notice that over the full range of φ , $x(T_s)$ is greater than $x(0)$ or $x(2T_s)$. Thus, if $y(T_s)$ is zero, $y(0)$ and $y(2T_s)$ cannot be D . This leaves four possible modes other than the trivial one. The four $y^*(t)$ waveforms are pictured in Fig. 9.2-8. Each of these modes is possible for a restricted range of φ which depends on the amplitude of the input. Take as an example the waveform *b*. The condition for $y(0) = D$ is

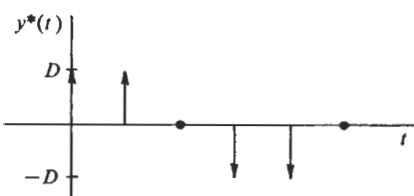
$$\begin{aligned} A \sin \varphi &> \delta \\ \text{or} \quad \varphi &> \Delta \end{aligned} \quad (9.2-36)$$

where we have defined

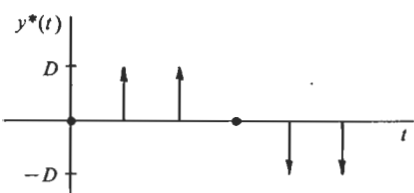
$$\Delta = \sin^{-1} \frac{\delta}{A} \quad (9.2-37)$$



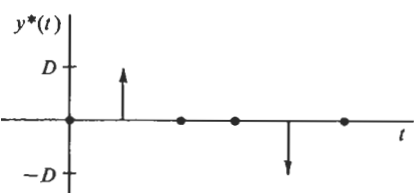
(a)



(b)



(c)



(d)

Figure 9.2-8 Possible modes for $T = 6T_s$.

The condition for $y(T_s) = D$ is

$$\Delta < \varphi + 60^\circ < 180^\circ - \Delta \quad (9.2-38)$$

and the condition for $y(2T_s) = 0$ is

$$\varphi + 120^\circ > 180^\circ - \Delta \quad (9.2-39)$$

The boundaries of these ranges of φ can be plotted against Δ , and a region in the φ, Δ space identified in which the conditions of Eqs. (9.2-36), (9.2-38), and (9.2-39) are simultaneously satisfied. This region is shown in Fig. 9.2-9 labeled (b). Also shown are the corresponding regions for the other waveforms of Fig. 9.2-8.

The describing function is now determined by calculating the fundamental component of each of the waveforms of Fig. 9.2-8. This is particularly easy to do since the harmonic analysis involves integrating functions which are sums of delta functions. The amplitude and phase relation between $x(t)$ and the fundamental component of $y^*(t)$ is then the sampled describing function, which is also $1/T_s$ times the z -transform describing function. For each of the modes of Fig. 9.2-8, this gives

$$(a) \quad N = \frac{4}{3} \frac{D}{AT_s} \angle 30^\circ - \varphi \quad (9.2-40a)$$

$$(b) \quad N = \frac{2}{\sqrt{3}} \frac{D}{AT_s} \angle 60^\circ - \varphi \quad (9.2-40b)$$

$$(c) \quad N = \frac{2}{\sqrt{3}} \frac{D}{AT_s} \angle -\varphi \quad (9.2-40c)$$

$$(d) \quad N = \frac{2}{3} \frac{D}{AT_s} \angle 30^\circ - \varphi \quad (9.2-40d)$$

The range of φ for which each of these modes can exist is given in terms of $\Delta = \sin^{-1}(\delta/A)$. Thus it is convenient to normalize N with δ and keep δ/A as the amplitude parameter. Limit cycle modes will be determined finally by plotting L versus $-1/N$; so the function $-1/N$ can best be plotted immediately.

$$(a) \quad \frac{D}{\delta T_s} \left(-\frac{1}{N} \right) = \frac{3}{4} \frac{A}{\delta} \angle \varphi - 210^\circ \quad (9.2-41a)$$

$$(b) \quad \frac{D}{\delta T_s} \left(-\frac{1}{N} \right) = \frac{\sqrt{3}}{2} \frac{A}{\delta} \angle \varphi - 240^\circ \quad (9.2-41b)$$

$$(c) \quad \frac{D}{\delta T_s} \left(-\frac{1}{N} \right) = \frac{\sqrt{3}}{2} \frac{A}{\delta} \angle \varphi - 180^\circ \quad (9.2-41c)$$

$$(d) \quad \frac{D}{\delta T_s} \left(-\frac{1}{N} \right) = \frac{3}{2} \frac{A}{\delta} \angle \varphi - 210^\circ \quad (9.2-41d)$$

Now, for every choice of A/δ in the range $(1, \infty)$, the magnitude of $-1/N$ in each mode is determined. Also, a range of phase angles for $-1/N$ is given by these expressions and the indicated range of φ in Fig. 9.2-9 at the value of $\Delta = \sin^{-1}(\delta/A)$. These describing function regions can conveniently be graphed on a gain-phase plot. Such a graph is shown for $T = 6T_s$ in Fig. 9.2-10. The regions within which the different modes exist are indicated. The possibility of a limit cycle of period $6T_s$ can be determined by evaluating the transfer function for the linear part of the system at the frequency $\frac{1}{6}\omega_s$.

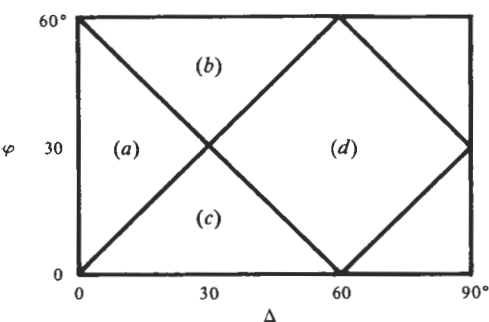


Figure 9.2-9 Regions of existence for the different modes.

multiplying it by $D/\delta T_s$, and noting the resulting complex number on this graph. If the point falls within one of the regions corresponding to a particular mode, the system can sustain that limit cycle mode. The indicated magnitude and phase of the describing function, together with the relations of Eqs. (9.2-41), then yield the amplitude and phase of the mode. If one desires to compensate the system to eliminate any or all limit cycle modes of this frequency, the necessary magnitude and phase of linear compensation at this frequency are obvious from the graph. Notice that in several regions more than one limit cycle mode can exist. Which mode a system will display, if any, depends on its initial conditions.

Calculation of the describing function for periods which are odd multiples of the sampling period is even more laborious than for even-multiple periods because no condition of symmetry such as Eq. (9.2-32) applies. This requires the value of $y(t)$ at each sampling point in the cycle to be considered independently, and gives rise to more possible modes. Some of these modes, which exist in different regions of the φ, Δ plane (corresponding to Fig. 9.2-9) map into the same describing function region (corresponding to Fig. 9.2-10). This occurs in the case of modes which have the same waveshape but are shifted in phase by one or more sampling periods or are traversed in the opposite direction.

In the case of even-multiple periods, all the possible $y^*(t)$ waveforms corresponding to unbiased sinusoidal inputs to the nonlinearity are unbiased functions. Both biased and unbiased waveforms are possible in the case of odd-multiple periods. However, only the unbiased modes are of consequence if $x(t)$ is assumed unbiased. If the linear part of the system includes an integrator (has a pole at the origin in the s plane), it is clear that $y^*(t)$ must be unbiased in any steady-state oscillation of the unexcited system. If the linear part has no pole at the origin, and also no zero, any bias in $y^*(t)$ would be propagated around the loop and appear at the nonlinearity input. Analysis of this situation would require two-input describing function theory. Only in the rare case of a linear part having a zero at the origin in the s

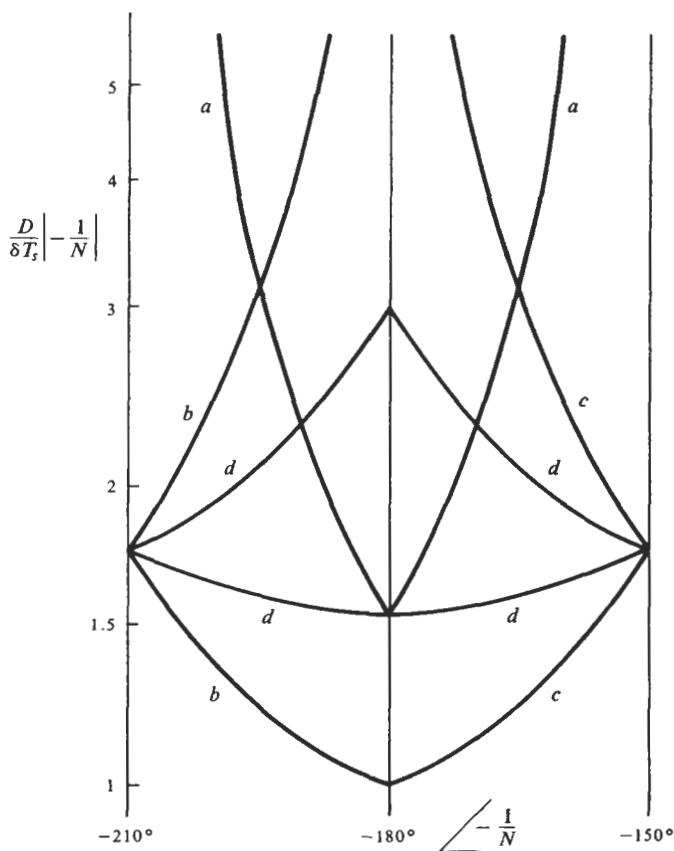


Figure 9.2-10 Sampled describing function for the three-level relay, $T = 6T_s$.

plane would a biased $y^*(t)$ waveform be consistent with an unbiased $x(t)$ for an unexcited system. Only the unbiased modes are included in the describing functions plotted in Appendix F.

Systems with a pole at the origin can sustain a biased output from the linear part even if the input to that part is unbiased. This leads to a range of possible null offsets, or bias levels in the nonlinearity input, which may remain uncorrected in the presence of any limit cycle mode. The situation in the case of the three-level relay is no different from that discussed earlier in the case of the two-level relay. Having determined the limit cycle modes which may exist under the assumption of an unbiased $x(t)$, the amplitude and phase angle of the sinusoid at $x(t)$ are known. Direct observation of

this sinusoid at the sampling points indicates how far the cycle may be biased up and down without changing the nonlinearity output. This defines the range of possible null offsets in the presence of a given limit cycle mode. It appears rather obvious, and is proved by Chow (Ref. 2), that no new unbiased $y^*(t)$ modes are introduced by the presence of a bias in $x(t)$.

The accuracy of describing function analysis applied to sampled nonlinear systems is of the same order as in the case of continuous systems. Many writers have done experimental studies to evaluate this accuracy. Among them are Chow (Ref. 2), Dixon (Ref. 5), and Kuo (Refs. 14, 15), all of whom report that for sampled three-level relay systems with second-order linear parts, the error in describing function prediction of the amplitude of limit cycle modes ranges generally from 1 to 10 percent. The critical value of system gain, or nonlinearity dead zone, δ , for the existence of a particular mode is even better predicted: the error is usually less than 5 percent. There is, in the case of sampled systems, no error in the determination of limit cycle frequency.

In calculating describing functions for the sampled three-level relay, the labor involved increases rapidly with the period of the limit cycle modes considered. At the same time, the importance of the sampling operation decreases as the period of the cycle increases. Thus, for long-period modes, an approximation to the describing function is both feasible and highly desirable. From the form of the describing functions plotted in Appendix F, one can anticipate the bounds on $-1/N$, which were derived by Chow (Ref. 2) and Russell (Ref. 23). If the period of the oscillation is $T = nT_s$, the negative reciprocal describing function exhibits phase angles within a band $2\pi/n$ wide for n even, or π/n wide for n odd, these bands being centered around the angle $-\pi$. The minimum magnitude of the function $-(D/\delta T_s)(1/N)$ is 0.5 for $n = 2$, is 1.0 for some small values of n , and approaches $\pi/2 = 1.57$ for large n . The maximum magnitude is always infinite. Thus, except for $n = 2$, for which the exact describing function is given in Appendix F, one can lay out a rectangle on the gain-phase plot ranging from 1.0 to infinity in amplitude and from $-\pi - \pi/n$ to $-\pi + \pi/n$ in phase, and be assured that $-(D/\delta T_s)(1/N)$ corresponding to all modes of period nT_s will lie within that rectangle. If the design requirement is to avoid any limit cycle modes, this bound on the describing function can be used to account for all modes of longer period than those for which the describing function has been calculated.

OTHER NONLINEARITIES

Describing function calculation for nonlinearities which have the same analytic description for all inputs is quite simple. Take as an illustration the cubic nonlinearity and sampler pictured in Fig. 9.2-11. Again, $x(t)$ is

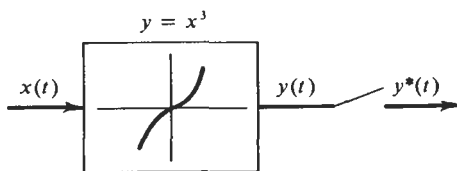


Figure 9.2-11 The sampled cubic nonlinearity.

taken to be a sinusoid as in Eq. (9.2-31). Thus

$$y(mT_s) = A^3 \sin^3(\omega mT_s + \varphi) \quad (9.2-42)$$

The fundamental component of $y^*(t)$ for $\omega = (1/n)\omega_s$ is

$$\begin{aligned} y^*(t)_f &= a \sin \omega t + b \cos \omega t \\ &= \sqrt{a^2 + b^2} \sin\left(\omega t + \tan^{-1} \frac{b}{a}\right) \end{aligned} \quad (9.2-43)$$

where

$$a = \frac{2}{nT_s} \int_0^{nT_s} y^*(t) \sin \frac{1}{n} \omega_s t dt$$

$$= \frac{2A^3}{nT_s} \sum_{m=0}^{n-1} \sin^3\left(\frac{m}{n} 2\pi + \varphi\right) \sin \frac{m}{n} 2\pi \quad (9.2-44)$$

and

$$b = \frac{2A^3}{nT_s} \sum_{m=0}^{n-1} \sin^3\left(\frac{m}{n} 2\pi + \varphi\right) \cos \frac{m}{n} 2\pi \quad (9.2-45)$$

The sampled describing function is then

$$N = \frac{1}{A} \sqrt{a^2 + b^2} / \tan^{-1}(b/a) - \varphi \quad (9.2-46)$$

The expressions for a and b can be reduced by trigonometric manipulations, but this will not be pursued here. The amplitude of the input in this case affects only the magnitude of N , which is proportional to A^2 . For any order n of limit cycle mode, $(1/A^2)N$ describes a closed contour in the complex plane or on a gain-phase plot as φ varies from 0 to $(1/n)2\pi$. This contour is then just scaled in magnitude with A^2 .

Lepschy and Ruberti (Ref. 16) have calculated the describing function for the dead-zone-gain nonlinearity with a sampler and zero-order hold. This nonlinearity is interesting not only in its own right, but also because parallel combinations of dead-zone gains can be used to synthesize any piecewise-linear continuous nonlinearity. As always, the sum of describing functions for the parallel elements is the describing function for the combination. To facilitate addition of the describing functions for dead-zone-gain elements, Lepschy and Ruberti have plotted their results, not only in terms of magnitude and phase, but also in terms of real and imaginary parts.

Some nonlinearities, such as the limiter, are of less interest in the study of limit cycles in sampled nonlinear systems than in continuous nonlinear systems because of the very rare occurrence of *stable* limit cycle modes of interesting form in systems containing these nonlinearities. The stability of indicated limit cycle modes is the subject of the next section.

9.3 STABILITY OF LIMIT CYCLE MODES

The analysis of the preceding sections has determined essentially the possible states of dynamic equilibrium of unexcited sampled nonlinear systems of a certain class. These equilibrium states, or limit cycles, can be either stable or unstable in that a small perturbation from the self-sustaining periodic mode may tend either to decay or grow. The determination of limit cycle modes simply identifies those signal histories which will reproduce themselves when propagated around a closed-loop system. This says nothing about the stability of the modes, or if stable, about the range of initial conditions which will result in eventual capture to a particular mode.

The standard technique of perturbation analysis to study the stability of limit cycles has even wider applicability to sampled than to continuous systems. In either case one supposes a small perturbation $p(t)$ to exist at the input to the nonlinearity, in addition to the limit cycle $x(t)$. The output of the nonlinearity is then expanded approximately into the limit cycle output plus a perturbation which is linearly related to $p(t)$. In the case of continuous systems, this expansion can be done only for nonlinearities which are differentiable over the range of inputs experienced in the limit cycle. This rules out such commonplace nonlinearities as two- and three-level relays. In the case of sampled systems, the nonlinearity need not be differentiable over any continuous range. The only points on the nonlinear characteristic which are of consequence are those at which the samples are taken in the limit cycle mode under consideration. Even in the case of discontinuous nonlinearities such as relays, the slope of the nonlinearity is well defined at those discrete points where the samples are taken in the limit cycle.

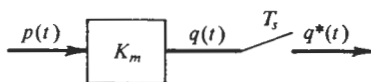
If the output of the nonlinearity can be expanded into the sum of the limit cycle output plus a perturbation which is linearly related to the input perturbation $p(t)$, the effect of the nonlinearity on the perturbation is characterized as a linear gain which depends on the limit cycle input $x(t)$, and hence is periodically time-varying. In the case of continuous systems, determination of the stability of linear systems containing a periodically time-varying gain is still a substantial chore. The same would be true of sampled systems, except that it is possible to transform the system from one containing a sampler with periodically varying gain into one containing multiple samplers with fixed gains in parallel. This complicates the configuration somewhat, but

permits the use of standard linear invariant theory to determine the stability of limit cycle modes.

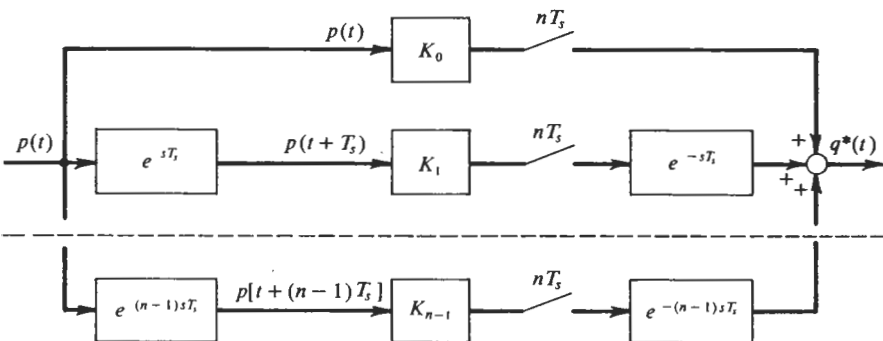
Nease (Ref. 18) proves that the stability of a periodic solution of a nonlinear set of difference equations is given by the stability of the linear set which approximates the action of the system on a small perturbation about the periodic solution. Nease also proves a theorem which establishes the stability of a linear set of difference equations with periodically varying coefficients. Because of its more likely appeal to control-system designers, we prefer to present here a technique for the study of stability suggested by Pyshkin (Ref. 21). Suppose that a sampled nonlinear system has been analyzed by the method of the preceding section, and the existence of a limit cycle of period $T = nT_s$ has been established. It remains to determine whether this indicated limit cycle is stable or unstable. If the periodic signal $x(t)$ which appears at the nonlinearity input in the steady-state limit cycle is perturbed by a small additive signal $p(t)$, the perturbation in the nonlinearity output at the sampling times, $q(mT_s)$, is given to first order by $p(mT_s)$ times the slope of the nonlinear characteristic dy/dx , evaluated at $x(mT_s)$. Considering the operation of the system on the perturbations only, the system configuration is the original configuration, with the nonlinearity replaced by the periodically time-varying gain $(dy/dx)[x(mT_s)]$. This gain is defined at the sampling instants only, but it is of consequence only at those instants.

The system whose stability determines the stability of the limit cycle contains one sampler (in addition to any samplers in the linear part of the original system), with sampling period T_s , preceded by a gain which takes a set of n discrete values at the sampling times and repeats them sequentially. This variable-gain sampler is indicated in Fig. 9.3-1a. Rather than deal with the stability of a variable-gain system, we prefer to replace the variable-gain sampler with n samplers in parallel, each having a fixed gain and the sampling period nT_s . The equivalent set of samplers is shown in Fig. 9.3-1b. Because ordinary sampled-data system analysis depends on the assumption that all samplers in the system operate synchronously, the various samplers in this equivalent configuration are preceded by ideal predictors, so that $p(t)$ will be sampled at the appropriate times, and followed by ideal delays, so that the samples will appear at the output at the correct times. With this transformation, the system whose stability determines the stability of the limit cycle under consideration becomes a fixed-parameter linear sampled-data system, and ordinary linear sampled-data system theory is applicable.

The characteristic equation of a system containing a parallel set of predictors, samplers, and delays, as in Fig. 9.3-1b, involves z transforms of functions with predictors or delays of a fraction of the sampling period. Such transforms can be found in tables of "modified z transforms" (Ref. 7) or "advanced z transforms" (Ref. 22). It should also be noted that if an



$$K_m = K_0, K_1, \dots, K_{n-1}, K_0, K_1, \dots$$

(a) Single sampler with pK_0 , dically varying gain(b) n samplers with fixed gains**Figure 9.3-1** Equivalent sampling systems.

unbiased even-period limit cycle mode (n even) is being tested for stability, and if the nonlinear characteristic is odd, then

$$\frac{dy}{dx} \left[x \left(mT_s + \frac{n}{2} T_s \right) \right] = \frac{dy}{dx} [x(mT_s)]$$

so the sequence of gains K_i , appearing in Fig. 9.3-1b, repeats after the first $n/2$ values. Thus only $n/2$ parallel paths are required, and each sampler operates with the period $(n/2)T_s$. These points can be illustrated by an example.

Example 9.3-1 Consider the sampled system containing a limiter shown in Fig. 9.3-2. The linear part includes a zero-order hold and an integrator. Test the stability of a limit cycle mode of period $T = 4T_s$, having the form $y(mT_s) = 1, a, -1, -a$ for $m = 0, 1, 2, 3$. The constant a can be any value between zero and 1.

First solution Just for illustration, work first with the full form of the equivalent sampling system for perturbation analysis as shown in Fig. 9.3-1b. The slope of the nonlinearity evaluated at the sampling points is

$$\frac{dy}{dx} [x(mT_s)] = 0, k, 0, k$$

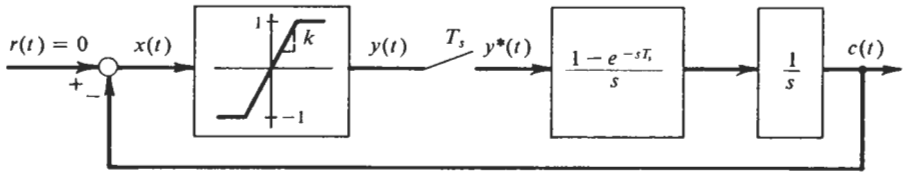


Figure 9.3-2 System for Example 9.3-1.

The full form of the linearly perturbed system is shown in Fig. 9.3-3. The characteristic equation for this system can be found in the following steps [$Q_i(s)$ is the Laplace transform of $q_i(t)$]:

$$Q_2 = -Q_2^* \frac{1 - e^{-sT_s}}{s^2} k - Q_4^* \frac{1 - e^{-sT_s}}{s^2} k e^{-2sT_s}, \quad (9.3-1)$$

$$Q_4 = -Q_2^* \frac{1 - e^{-sT_s}}{s^2} k e^{2sT_s} - Q_4^* \frac{1 - e^{-sT_s}}{s^2} k$$

Equivalently,

$$(1 + F_1^*)Q_2^* + F_2^*Q_4^* = 0 \quad (9.3-2)$$

$$F_3^*Q_2^* + (1 + F_1^*)Q_4^* = 0$$

where

$$F_1^* = k \left(\frac{1 - e^{-sT/4}}{s^2} \right)^* \quad (9.3-3)$$

$$F_2^* = k \left(\frac{1 - e^{-sT/4}}{s^2} e^{-sT/2} \right)^*$$

$$F_3^* = k \left(\frac{1 - e^{-sT/4}}{s^2} e^{sT/2} \right)^*$$

The star indicates the z transform with respect to the sampling period $T = 4T_s$. As an illustration of this calculation, find the transform F_2^* .

$$\begin{aligned} F_2^* &= k \left(\frac{e^{-sT/2}}{s^2} - \frac{e^{-s\frac{3}{2}T}}{s^2} \right)^* \\ &= k \left(e^{-sT} \frac{e^{sT/2}}{s^2} - e^{-sT} \frac{e^{s\frac{3}{2}T}}{s^2} \right)^* \end{aligned}$$

This transform is found directly in a table of modified or advanced z transforms.

$$\begin{aligned} F_2^* &= k \left[z^{-1} \frac{\frac{1}{2}T + \frac{1}{2}Tz^{-1}}{(1 - z^{-1})^2} - z^{-1} \frac{\frac{3}{2}T + \frac{3}{2}Tz^{-1}}{(1 - z^{-1})^2} \right] \\ &= \frac{kT_s}{z - 1} \quad (9.3-4) \end{aligned}$$

Similarly, one finds

$$F_1^* = \frac{kT_s}{z - 1} \quad (9.3-5)$$

$$F_3^* = \frac{kT_s z}{z - 1} \quad (9.3-6)$$

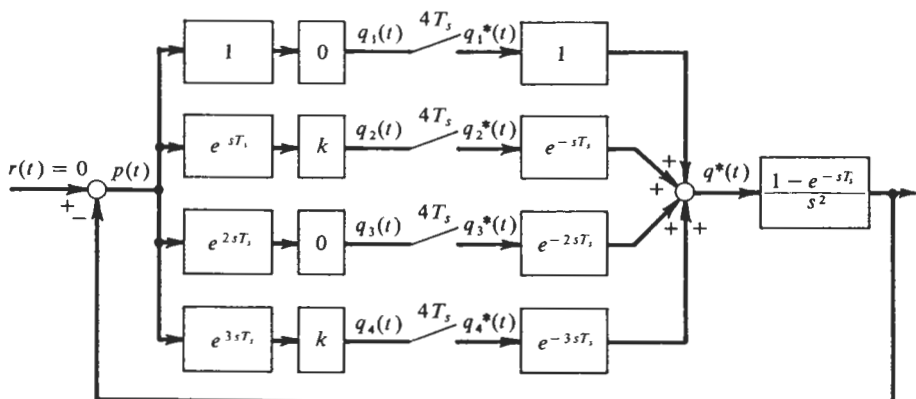


Figure 9.3-3 Full form of perturbed system of Example 9.3-1.

The characteristic equation of this system results from equating to zero the determinant of the coefficient matrix in Eqs. (9.3-2).

$$(1 + F_1^*)^2 - F_2^* F_3^* = 0$$

With Eqs. (9.3-4) to (9.3-6) this becomes

$$z = (1 - kT_s)^2 \quad (9.3-7)$$

The closed-loop pole takes values between 0 and 1 for values of kT_s in the range

$$0 < kT_s < 2$$

This is the range of stability for the linearly perturbed system. Thus, if the original system had an indicated limit cycle mode of the stated form for a value of kT_s in this range, the mode would be stable.

Second solution The analysis of this problem can be simplified because the limit cycle under consideration is an unbiased even-period mode and the nonlinearity is odd. Thus, only the first half of the parallel paths shown in Fig. 9.3-3 are needed if the period of the samplers is changed to $2T_s$. But this leaves only one path with a nonzero gain. This is the second path, which includes a one-unit predictor and a one-unit delay. With just a single path, a predictor and corresponding delay have no effect on system stability, and for the present purpose can be ignored. If there were multiple paths of this form, all predictors and delays could be shifted by the same time interval with no effect on the stability of the system.

The simplified form of the perturbed system is shown in Fig. 9.3-4. This is just an ordinary single-path linear sampled-data system formed from the original nonlinear system by replacing the limiter by its gain in the linear region and changing the sampling period from T_s to $2T_s$. The closed-loop root of this system is found to be located at

$$z = 1 - kT_s \quad (9.3-8)$$

Again the stable range is found to be

$$0 < kT_s < 2$$

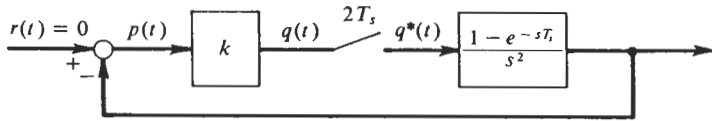


Figure 9.3-4 Simplified form of perturbed system of Example 9.3-1.

At the unstable boundary, $kT_s = 2$, the closed-loop pole in this case is located at $z = -1$, which implies a characteristic mode whose samples oscillate between constant plus and minus values. In the previous case, Eq. (9.3-7) shows the closed-loop pole to be located at $z = +1$ for $kT_s = 2$. This pole location implies a characteristic mode whose samples are all the same constant value. This is not an inconsistency since z in Eq. (9.3-8) is e^{s2T_s} , whereas z in Eq. (9.3-7) is e^{s4T_s} . The mode which oscillates between equal plus and minus values every $2T_s$ displays the same constant value when sampled every $4T_s$.

This example shows why limiters are somewhat uninteresting for limit cycle analysis of sampled nonlinear systems. If the system is designed to be stable within the linear range of the limiter, it is unusual for limit cycle modes of the partially saturated type considered in the example to exist. But if the gain or sampling period is increased to the point where such a mode does exist, it is quite likely that the system is unstable in the linear range with the sampling period T_s ; it is very rare that the system would be found stable with the sampling period $2T_s$ as required for stability of the limit cycle mode. Thus, for most limiter systems, the only *stable* limit cycle modes found are the fully saturated modes, in which the limiter acts just like a two-level relay.

One may also note the simple interpretation of this stability analysis in the case of *two- or three-level relay systems*. Since the slope of these nonlinear characteristics at any sampling point is zero, the linearized system which processes perturbations on any limit cycle mode has a gain preceding the sampler which is zero at every sampling instant. Thus, as far as perturbations are concerned, there is no loop closed around the linear part of the system. These modes are then stable if the open-loop linear part is stable, and unstable if the open-loop linear part is unstable.

9.4 EXACT VERIFICATION OF LIMIT CYCLE MODES

In Sec. 9.2 we discussed two points of view regarding the determination of possible limit cycle modes in sampled nonlinear systems, each depending on the describing function approximation that the input to the nonlinearity is a sinusoid. This approximation is a good one if the system has sufficient linear filtering of the harmonics generated by the nonlinearity and by the samplers. For the great majority of practical purposes, "sufficient" linear filtering is provided by second- or higher-order filters if the fundamental frequency is near or beyond the cutoff frequency of the filter.

In those cases in which one questions the adequacy of the linear filtering properties of a system for describing function analysis, he can verify exactly whether or not any suggested limit cycle can exist. Indeed, if one wishes, he can use an exact technique as his basic tool for limit cycle determination in the first place. The only objection to this is the greater labor involved and the uncertainty regarding how many possible modes to test. Using an exact technique, the test to determine whether or not any suggested limit cycle mode can exist in a system is an individual problem; it must be repeated for every suggested mode and for every system to be considered. The virtue of the describing function approach is that it allows separate characterization of the linear and nonlinear parts of the system. A particular nonlinearity can be considered quite independent of any system, and its describing function calculated for any number of modes. With these functions in hand, very likely graphed, one then need consider only the transfer characteristics of the linear parts of any systems which contain this nonlinearity to determine the existence of all the modes for which the describing function was originally calculated. In addition, the form of the describing function for the different modes considered, and the shape of the frequency response function for the linear part, often make it clear whether or not other modes are likely to exist.

The procedure for testing the existence of a suggested mode is simple and obvious in principle. The mode to be tested is characterized by a particular periodic sequence of samples at the nonlinearity output. This sequence is the input to the linear part of the system; together with the unknown initial conditions in the linear part, it determines the output of the linear part. But this output is the input to the nonlinearity. If a set of initial conditions can be found which in the steady state will produce a nonlinearity input consistent with the nonlinearity output originally assumed, this will demonstrate the possible existence of the mode. Simple input forms, such as steps and fundamental frequency sinusoids, can also be included in this analysis. Many writers have employed this procedure, the differences in their approaches being in the technique used to propagate the assumed nonlinearity output through the linear part and the means of handling the initial and steady-state conditions. Bergen (Ref. 1) suggested use of the Laplace transform of $y^*(t)$ and the transfer function for the linear part to get the Laplace transform of $x(t)$, including initial-condition terms. The z transform of this expression was taken, and the initial conditions chosen to eliminate the transient term, thus revealing the desired steady-state solution. Jury and Nishimura (Ref. 8) use z -transform theory to accumulate the incremental responses of the linear part to each impulse of $y^*(t)$, employ skip sampling to select the corresponding sampled value of $x(t)$ in each period of the cycle, and apply the final-value theorem to determine the steady-state values of these samples. Special consideration must be given to the possible bias level which can exist in the case of systems with an

integrator. Pai (Ref. 19) described the use of the z transform of the specified $y^*(t)$ and of the sampled transfer function for the linear part to calculate the z transform of $x(t)$. He also prescribed the form of the z transform of the steady-state oscillation at $x(t)$, and equated coefficients of like powers of z to derive the algebraic equations to be solved simultaneously for the samples of $x(t)$. Torng and Meserve (Refs. 17, 26) first expand the periodic sequence of samples of $y(t)$ into a series of orthogonal functions; they used sines and cosines with integral arguments. Using the difference equation for the linear part, they then solve for the coefficients in the expansion of the periodic sequence of samples of $x(t)$. Having these coefficients, the samples themselves are determined. No account need be taken of initial conditions since the samples of $y(t)$ and $x(t)$ are taken in the form of steady-state periodic sequences at the outset. Torng (Ref. 25) later suggested use of complex exponentials as the basis for the series expansion. Such an expansion is, in effect, a Fourier transformation, and the coefficients in the expansion enjoy a multiplicative input-output relation for linear systems.

Of all known techniques, two are described here as being perhaps the most direct. The most straightforward approach, conceptually, is the direct use of the difference equation for the linear part to write down a set of algebraic equations which determine the samples of $x(t)$. Interestingly enough, none of the writers referred to above used this procedure. The resulting equations must be solved simultaneously, but most of the procedures mentioned above lead to the same equations to be solved. The second technique described uses the "transform" of the $y^*(t)$ and $x^*(t)$ sequences, or their expansion into series of complex exponentials. This procedure does not require solution of equations; it is a direct, step-by-step calculation. However, the calculation requires a great deal of complex algebra, and it is not clear that the labor involved is less than in the case of the first procedure. It should be emphasized that any of these procedures give only necessary conditions for the existence of a limit cycle mode. Whether or not such a mode will actually be observed depends first of all upon whether the mode is stable or unstable; and if stable, it depends on the system initial conditions.

THE DIFFERENCE EQUATION METHOD

The object of our present endeavor is to see whether a postulated periodic sequence of samples of $y(t)$, the nonlinearity output, will result in a sequence of samples of $x(t)$, the nonlinearity input, which in the steady state will reproduce the postulated $y^*(t)$. Having the samples of $y(t)$ given, the most obvious way to calculate the samples of $x(t)$ is to make direct use of the difference equation for the linear part, which is evident from the z transform of its transfer function. This, in one sentence, is a complete description of the procedure. We proceed to an illustration.

Example 9.4-1 An example used to illustrate the sampled describing function and z -transform describing function techniques will be used here as well. This will afford an exact check on the results derived by the describing functions. The system under consideration is that of Example 9.2-2, for which the configuration is shown in Fig. 9.2-6. The question posed is the determination of the range of values of a , the parameter of the digital lead compensator, for which the 3, 3 limit cycle mode is impossible.

The postulated sequence of nonlinearity output samples is $y(mT_s) = D, D, D, -D, -D, -D$ for $m = 0, 1, 2, 3, 4, 5$. For simplicity, $y(mT_s)$ will hereafter be denoted y_m . This sequence is periodically repeating:

$$y_{m+6} = y_m \quad (9.4-1)$$

The sampled transfer function for the system linear part is

$$\begin{aligned} \frac{X(z)}{Y(z)} &= -K \left[\frac{(1 - az^{-1})(1 - z^{-1})}{s^2(\tau s + 1)} \right]^* \\ &= -KT_s \left[\frac{z - b - (\tau/T_s)(1 - b)(z - 1)}{(z - 1)(z - b)} \right] \frac{z - a}{z} \end{aligned} \quad (9.4-2)$$

using the notation

$$b = e^{-T_s/\tau} \quad (9.4-3)$$

As in Example 9.2-2, take $T_s/\tau = 1$. Then Eq. (9.4-2) implies the difference equation

$$x_m - 1.368x_{m-1} + 0.368x_{m-2} = -KT_s[0.368y_{m-1} + (0.264 - 0.368a)y_{m-2} - 0.264ay_{m-3}] \quad (9.4-4)$$

which holds for all m . The y_m are given for all m , and using the periodicity relation, [Eq. (9.4-1)], which holds for the x_m as well as for the y_m , one can let m take the values 0, 1, 2, ..., 5 in Eq. (9.4-4) and write down six relations among the six unknowns x_0 to x_5 .

$$\begin{aligned} x_0 - 1.368x_5 + 0.368x_4 &= -KDT_s(-0.632 + 0.632a) \\ x_1 - 1.368x_0 + 0.368x_5 &= -KDT_s(0.104 + 0.632a) \\ x_2 - 1.368x_1 + 0.368x_0 &= -KDT_s(0.632 - 0.104a) \\ x_3 - 1.368x_2 + 0.368x_1 &= -KDT_s(0.632 - 0.632a) \\ x_4 - 1.368x_3 + 0.368x_2 &= -KDT_s(-0.104 - 0.632a) \\ x_5 - 1.368x_4 + 0.368x_3 &= -KDT_s(-0.632 + 0.104a) \end{aligned} \quad (9.4-5)$$

These equations do not yield a unique solution for the x_m since only five are linearly independent. Thus five of the x_m can be expressed in terms of the sixth. If one solves for x_0 to x_4 , the result is

$$\begin{aligned} x_0 &= x_5 - KDT_s(-0.837 + 0.557a) > 0 \\ x_1 &= x_5 - KDT_s(-1.041 + 1.393a) > 0 \\ x_2 &= x_5 - KDT_s(-0.484 + 1.599a) > 0 \\ x_3 &= x_5 - KDT_s(0.354 + 1.043a) < 0 \\ x_4 &= x_5 - KDT_s(0.558 + 0.204a) < 0 \\ x_5 & < 0 \end{aligned} \quad (9.4-6)$$

The inequalities on the right have been added as the conditions required to sustain the postulated y_m sequence. The easiest way to interpret these six conditions is to plot the boundaries between admissible and inadmissible values of x_5 as functions of a . The conditions on x_2 and x_5 are found to conflict if $a > 0.303$. The conditions on x_0 and x_3 conflict if $a < -2.45$. Thus

$$-2.45 < a < 0.303$$

is the range of values of a for which the 3, 3 limit cycle mode is possible in this system. Values of a outside this range render the mode impossible, either because of too much lead in the linear part or too much lag. These boundaries on the range of a may be compared with -2.46 , 0.289 , derived using the sampled describing function, and -2.54 , 0.283 , obtained with the z -transform describing function. The errors in these describing function results range from 0.4 to 6.6 percent.

For values of a within the range from -2.45 to 0.303 , there is a range of values of x_5 for which all the inequalities of Eqs. (9.4-6) are satisfied. This range of freedom for x_5 , and thus for all the x_m , represents the range of possible bias levels which can exist in $x(t)$ in the presence of the 3, 3 limit cycle mode. For example, if there were no digital lead, $a = 0$, the 3, 3 mode would be possible and x_5 could take values ranging from 0 to $-0.484KDT_s$. The symmetrical limit cycle would have $x_5 = -0.242KDT_s$, and the null offset or bias could range between $\pm 0.242KDT_s$.

In the case of an even-period mode such as this, a simpler procedure can be employed. The critical condition for the existence of a limit cycle mode always occurs for the unbiased, or symmetrical, mode. If the symmetry condition is postulated,

$$x_{m+3} = -x_m \quad (9.4-7)$$

just three of the x_m define the mode, and there is no remaining uncertainty due to bias level. Using Eq. (9.4-7) in the first three of Eqs. (9.4-5),

$$\begin{aligned} x_0 + 1.368x_2 - 0.368x_1 &= -KDT_s(-0.632 + 0.632a) \\ x_1 - 1.368x_0 - 0.368x_2 &= -KDT_s(0.104 + 0.632a) \\ x_2 - 1.368x_1 + 0.368x_0 &= -KDT_s(0.632 - 0.104a) \end{aligned} \quad (9.4-8)$$

These equations have a unique solution. Each of these x_m must be greater than zero to reproduce the postulated y_m sequence. The critical conditions are

$$\begin{aligned} x_0 &= KDT_s(0.595 + 0.243a) > 0 \\ x_2 &= KDT_s(0.242 - 0.799a) > 0 \end{aligned} \quad (9.4-9)$$

which again gives $-2.45 < a < 0.303$ as the condition for the existence of the 3, 3 mode. For values of a in this range, the mode is possible, and the possible range of bias levels is evident.

THE TRANSFORM METHOD

This is the technique described by Torng (Ref. 25). It centers attention not on the sequences of samples of $y(t)$ and $x(t)$ directly, but rather on the coefficients of the expansions of these sequences into series of complex exponentials with integral arguments. The virtue of this is the fact that a periodic sequence can be processed through a linear discrete filter more readily in terms of these coefficients than in terms of the sequences themselves,

since a multiplicative input-output relation exists for the coefficients. In this and all other respects, a direct analogy exists between this theory and the familiar Fourier transform theory for continuous functions and systems.

A discrete sequence of n values,

$$y_m = y_0, y_1, \dots, y_{n-1} \quad (9.4-10)$$

which repeats periodically with the period n , can be expressed as a series of n complex exponential terms.

$$y_m = \sum_{l=-k}^{k+1} Y_l \exp \left(j l \frac{2\pi}{n} m \right) \quad (9.4-11)$$

where k is defined by

$$n = \begin{cases} 2k + 1 & n \text{ odd} \\ 2k + 2 & n \text{ even} \end{cases} \quad (9.4-12)$$

and the convention $Y_{k+1} = 0$ if n is odd will be observed. The coefficients in this expansion, or transformation, are given by

$$Y_l = \frac{1}{n} \sum_{m=0}^{n-1} y_m \exp \left(-j l \frac{2\pi}{n} m \right) \quad (9.4-13)$$

From this expression we note the property

$$Y_{-l} = Y_l^* \quad (9.4-14)$$

so the coefficients with negative indices need not be calculated separately.

If this periodic sequence y_m is the input to a discrete linear filter, and x_m is the output, and if this filter has the sampled transfer function $D(z)$,

$$\frac{X(z)}{Y(z)} = D(z) \quad (9.4-15)$$

then the coefficients of the expansion of the x_m sequence are given by

$$X_l = D \left[\exp \left(j l \frac{2\pi}{n} \right) \right] Y_l \quad (9.4-16)$$

If the modified or advanced z transform for the linear filter is used in this relation for X_l , then the entire $x(t)$ history is defined by the inverse transform [Eq. (9.4-11)].

The procedure for testing the existence of a postulated limit cycle mode using the transform method is then to transform the postulated y_m sequence, using Eq. (9.4-13), and to calculate the X_l coefficients from Eq. (9.4-16) and the x_m sequence from Eq. (9.4-11). The conditions on the x_m which will sustain the postulated y_m sequence can then be applied. Steady-state conditions are assumed throughout, since the form of the transformation is applicable only to periodic sequences, and the input-output relation for linear systems gives the forced response only.

Example 9.4-2 Repeat Example 9.4-1, using the transform method. The y_m sequence to be tested is

$$y_m = D, D, D, -D, -D, -D \quad (9.4-17)$$

which repeats with period $n = 6$. According to Eq. (9.4-12), $k = 2$ in this case. Y_l must be calculated for $l = 0, 1, 2, 3$, according to Eq. (9.4-13). As an illustration of this calculation, consider Y_1 .

$$\begin{aligned} Y_1 &= \frac{D}{6} \left[1 + \exp\left(-j\frac{\pi}{3}\right) + \exp\left(-j\frac{\pi}{3}2\right) \right. \\ &\quad \left. - \exp\left(-j\frac{\pi}{3}3\right) - \exp\left(-j\frac{\pi}{3}4\right) - \exp\left(-j\frac{\pi}{3}5\right) \right] \\ &= \frac{D}{3} \left[1 + \exp\left(-j\frac{\pi}{3}\right) + \exp\left(-j\frac{2\pi}{3}\right) \right] \\ &= \frac{D}{3} (1 - j\sqrt{3}) \end{aligned} \quad (9.4-18)$$

The other Y_l are computed in the same way.

$$\begin{aligned} Y_0 &= 0 \\ Y_2 &= 0 \\ Y_3 &= \frac{D}{3} \end{aligned} \quad (9.4-19)$$

The sampled transfer function for the linear part of this system is found from Eq. (9.4-2), using Eq. (9.4-3) and $T_s/\tau = 1$, to be

$$\frac{X}{Y}(z) = \frac{-KT_s[0.368z^2 + (0.264 - 0.368a)z - 0.264a]}{z^3 - 1.368z^2 + 0.368z} \quad (9.4-20)$$

The X_l are now calculated from Eq. (9.4-16). Take X_1 as an illustration.

$$\begin{aligned} X_1 &= \frac{X}{Y} \left[\exp\left(j\frac{\pi}{3}\right) \right] Y_1 \\ &= \frac{-KT_s[0.368 \exp(j2\pi/3) + (0.264 - 0.368a) \exp(j\pi/3) - 0.264a][(D/3)(1 - j\sqrt{3})]}{\exp(j\pi) - 1.368 \exp(j2\pi/3) + 0.368 \exp(j\pi/3)} \\ &= 0.435KDT_s[0.670 + 0.264a + j(-0.691 + 0.926a)] \end{aligned} \quad (9.4-21)$$

Needless to say, a fair amount of algebra has been omitted between these last steps. X_2 and X_3 are calculated in the same way.

$$\begin{aligned} X_2 &= 0 \\ X_3 &= 0.0127KDT_s(1 + a) \end{aligned} \quad (9.4-22)$$

The expression for X_0 , however, is indeterminate.

$$\begin{aligned} X_0 &= \frac{X}{Y}(1)Y_0 \\ &= \frac{0}{0} \end{aligned} \quad (9.4-23)$$

X_0 will be carried as an unknown coefficient. This is the manifestation of the undetermined bias level which can exist in the presence of the limit cycle.

The x_m sequence can now be calculated from Eq. (9.4-11), using the property $X_{-l} = X_l^*$.

$$\begin{aligned} x_m &= 0.435KDT_s [0.670 + 0.264a - j(-0.691 + 0.926a)] \exp\left(-j\frac{\pi}{3}m\right) \\ &+ X_0 + 0.435KDT_s [0.670 + 0.264a + j(-0.691 + 0.926a)] \exp\left(j\frac{\pi}{3}m\right) \\ &+ 0.0127KDT_s(1+a) \exp(j\pi m) \\ &= 0.435KDT_s \left[\frac{2.30}{KDT_s} X_0 + 0.0291(-1)^m(1+a) \right. \\ &\left. + 2 \operatorname{Re} \left\{ [0.670 + 0.264a + j(-0.691 + 0.926a)] \exp\left(j\frac{\pi}{3}m\right) \right\} \right] \end{aligned} \quad (9.4-24)$$

Substitution of the various values of m in this expression yields the required results.

$$\begin{aligned} x_0 &= KDT_s \left(\frac{X_0}{KDT_s} + 0.595 + 0.243a \right) > 0 \\ x_1 &= KDT_s \left(\frac{X_0}{KDT_s} + 0.797 - 0.596a \right) > 0 \\ x_2 &= KDT_s \left(\frac{X_0}{KDT_s} + 0.242 - 0.799a \right) > 0 \\ x_3 &= KDT_s \left(\frac{X_0}{KDT_s} - 0.595 - 0.243a \right) < 0 \\ x_4 &= KDT_s \left(\frac{X_0}{KDT_s} - 0.797 + 0.596a \right) < 0 \\ x_5 &= KDT_s \left(\frac{X_0}{KDT_s} - 0.242 + 0.799a \right) < 0 \end{aligned} \quad (9.4-25)$$

Except for the X_0 terms, these relations are identical with those derived by the difference equation method under the assumption of a symmetrical limit cycle, and they define the same range of values of a for which the postulated mode is possible.

Application of either of these exact methods of determining or verifying the existence of limit cycle modes is considerably more tedious than use of the describing function techniques discussed in Sec. 9.2, especially the sampled describing function. An exact technique would ordinarily be required only when one has reason to question describing function results. Lack of sufficient continuous linear filtering is the primary reason for such a question. Another reason is a marginal situation in which a system design is near the boundary between possibility and impossibility for a particular

mode. Regardless of how the necessary conditions for existence of a limit cycle are established, the theory of Sec. 9.3 can be applied to test the stability of the mode.

9.5 LIMIT CYCLES IN PULSE-WIDTH-MODULATED SYSTEMS

A control system employing a pulse-width modulator, hereafter abbreviated PWM, is a special case of a sampled nonlinear system, and the techniques of the preceding sections can readily be applied to such a system. The primary reason for the utilization of a PWM in a control system is to achieve an approximation to proportional control in spite of a drive system which is only capable of—or for some reason is employed in—an on-off mode of operation. Somewhat varying forms of pulse-width modulators have been used, but the most common form is the linear lead modulator, which will be considered for the purpose of illustration here. The operation of this modulator is pictured in Fig. 9.5-1, and is defined by the following relations, which hold for all $m = 0, 1, 2, \dots$:

$$y(t) = \begin{cases} D \operatorname{sgn} [x(mT_s)] & mT_s < t < mT_s + k |x(mT_s)| \\ 0 & mT_s + k |x(mT_s)| < t < (m + 1)T_s \end{cases} \quad (9.5-1)$$

if $k |x(mT_s)| < T_s$. Otherwise,

$$y(t) = D \operatorname{sgn} [x(mT_s)] \quad mT_s < t < (m + 1)T_s \quad (9.5-2)$$

if $k |x(mT_s)| > T_s$.

Possible variations on this form of PWM are of two types. First, the relation between the sampled value of $x(t)$ and the pulse width may be any well-defined relation whatever, rather than the proportional relation considered here. Second, the zero interval in each sampling period of $y(t)$ may be placed in the first part of each period, with the nonzero interval following in the second part. This is known as a lag PWM. Neither of these variations complicates the application of the analytic techniques discussed here. In any case, even if the relation between $x(mT_s)$ and pulse width is linear, and if the possibility of saturation is ignored, the PWM operation is a nonlinear operation, and a nonlinear theory must be employed to study the details of the performance of a system using a PWM.

A number of writers have detailed various approaches to the exact determination of limit cycles in PWM systems. The same point of view is used as in the case of other sampled nonlinear systems: the form of limit cycle mode is postulated, which defines the form of the nonlinearity output; this

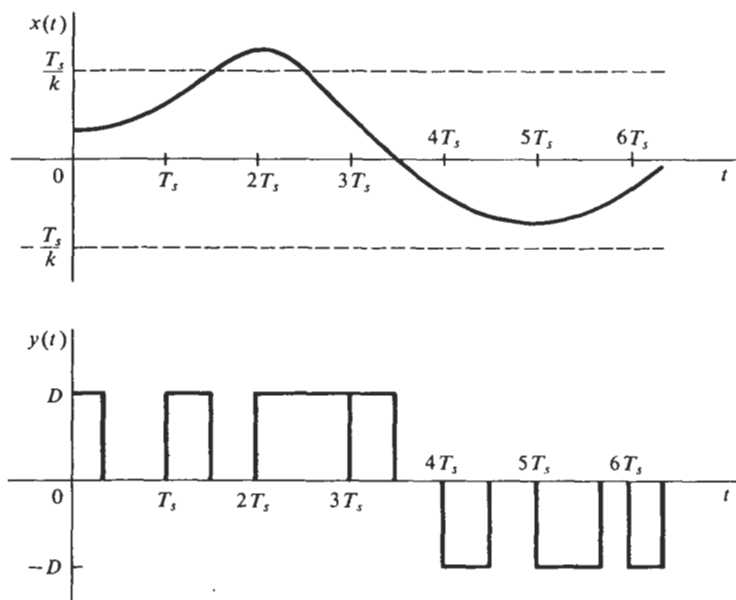


Figure 9.5-1 Operation of a linear lead PWM.

signal form is processed through the linear part of the system to the nonlinearity input; and conditions are applied which will produce the postulated output of the nonlinearity. Da-Chuan (Ref. 3) implemented this procedure for limit cycles of period $T = 2T_s$, using time response expressions directly. The procedure of Jury and Nishimura (Ref. 8), which was described in the preceding section in connection with other sampled nonlinear systems, can be applied equally well to PWM systems. Nease (Ref. 18) included PWM systems in his development of exact methods and general principles applicable to sampled nonlinear systems. The difference equation and transform methods described in Sec. 9.4 are not directly applicable to PWM systems because the input to the linear part of the system in this case is not a periodic train of impulses. However, direct time response, z transform, and Laplace transform techniques can all be used to calculate the response of the linear part to an input train of variable-width pulses.

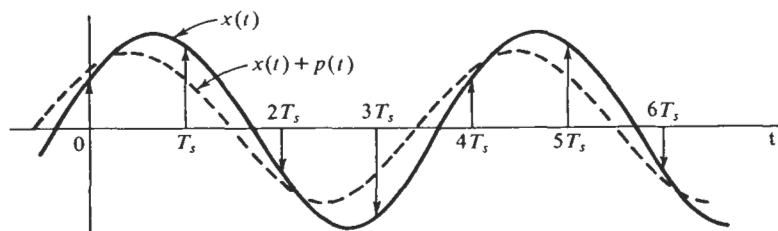
The describing function point of view can be applied to PWM systems in essentially the same way as it is applied to other sampled nonlinear systems. Delfeld and Murphy (Ref. 4) did this in an unnecessarily complicated way. Pyshkin (Ref. 21) took the straightforward approach, and treated limit cycles with periods $2T_s$ and $4T_s$. Calculation of the describing function for any particular form of PWM, such as the linear lead PWM considered for an illustration here, is quite simple in principle, the detail becoming tedious for

large-period modes because of the different modal forms of the same period which occur for different values of amplitude and sampling phase. The input to the modulator is taken in the standard form

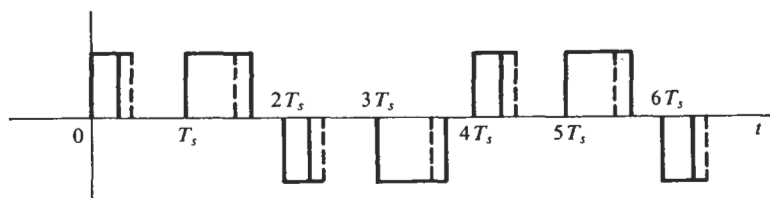
$$x(t) = A \sin(\omega t + \varphi) \quad (9.5-3)$$

with the time origin chosen at one of the sampling points. The frequencies of interest in limit cycle analysis are whole fractions of the sampling frequency—and in fact, just the even fractions, since one would not anticipate odd-period modes in a PWM system, especially if the linear part includes an integration. For any chosen frequency, the output of the PWM corresponding to any pair of values for A , φ is defined, and the fundamental harmonic component of this waveform is readily computed. Thus the describing function of the PWM is defined as a function of the ratio of the sinusoidal frequency to the sampling frequency, the amplitude of the input sinusoid, and the phase of that sinusoid relative to the sampling points. The negative reciprocal describing function for the linear lead PWM defined by Eqs. (9.5-1) and (9.5-2) is plotted in Appendix F for sinusoidal periods of 2, 4, 6, and 8 sampling periods. The possible existence of a limit cycle mode in a PWM system may be determined by placing the point corresponding to the transfer function for the linear part of the system, evaluated at fundamental frequency, on one of these plots. If the point lies within the region spanned by the describing function curves, one or more modes of that period are possible, and the corresponding amplitude and phase may be found by interpolation among the curves.

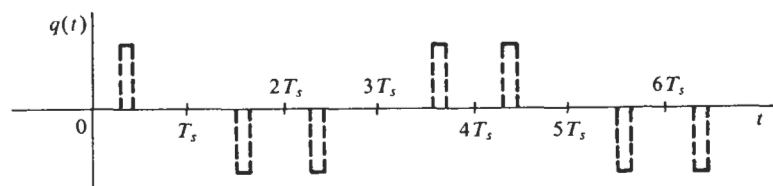
Any limit cycle found possible should be tested for stability. The technique described in Sec. 9.3 in relation to other sampled nonlinear systems can be applied, with a slight change of concept, to the present case as well. Consider a limit cycle $x(t)$ to experience a small additive perturbation $p(t)$. The output of the PWM is then a series of pulses with widths slightly perturbed from the pulse widths in the limit cycle. If the limit cycle signal at $y(t)$ is subtracted from this perturbed signal, the remaining perturbation $q(t)$ is a series of narrow pulses occurring near the ends of the pulses in the limit cycle. These signals are pictured in Fig. 9.5-2. In view of the fact that PWM systems are usually designed with a sampling period short compared with the response time of the linear part of the system, so the ripple at sampling frequency is well attenuated at the output of the system, the pulses in the output perturbation shown in Fig. 9.5-2c are very narrow compared with the linear-part response time, and can properly be approximated as impulses of the same area. The relation between input perturbation and output perturbation approximated as a sequence of impulses occurring at the ends of the pulses in the unperturbed limit cycle can then be linearized. In general, this requires the slope of the function which relates sampled input magnitude to pulse width. For the linear function of Eq.



(a) PWM input: limit cycle plus perturbation



(b) PWM output: limit cycle plus perturbation



(c) Perturbation at PWM output

Figure 9.5-2 Operation of a PWM with a perturbed limit cycle input.

(9.5-1), this slope is just k if the pulse is unsaturated, or zero if the pulse is saturated. If this slope, evaluated at the unperturbed limit cycle point $x(mT_s)$, is called K_m , then the perturbation $p(mT_s)$ gives rise to an approximate impulse of area $p(mT_s)K_mD$, occurring at the end of the pulse corresponding to $x(mT_s)$.

This linearized relation between input and output perturbations can now be represented by a parallel set of phased samplers with fixed gains, as was done in Sec. 9.3. For a limit cycle of period $T = nT_s$, where n is an even integer, $n/2$ such samplers are required, each with the sampling period $\frac{1}{2}nT_s$. The configuration is shown in Fig. 9.5-3. This linearized representation of the operation of the PWM on perturbations added to a limit cycle can be used with the transfer function for the linear part of the system to define a linear fixed-parameter sampled-data system whose stability determines the stability of the limit cycle under consideration. It may be noted that the gain K_m

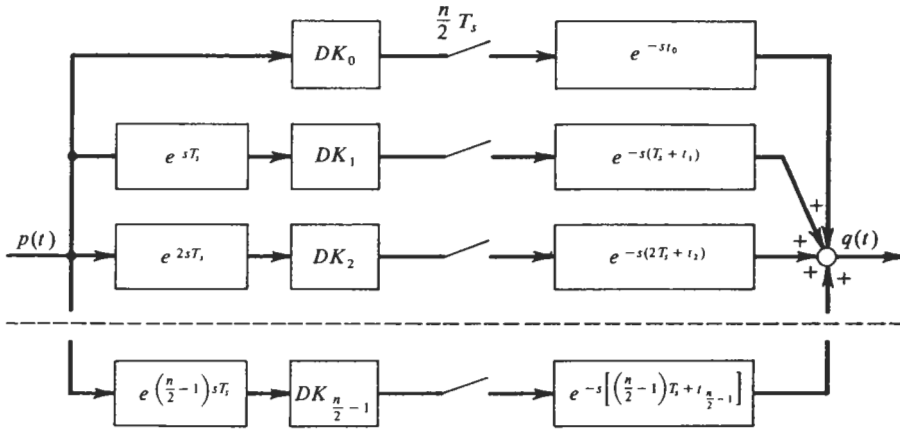


Figure 9.5-3 Linearized equivalent of PWM for perturbation analysis.

K_m = slope of function relating input magnitude to pulse width, evaluated at the limit cycle value $x(mT_s)$.

t_m = pulse width corresponding to the limit cycle value $x(mT_s)$.

associated with any saturated pulse is zero, and in effect the corresponding path is omitted from the configuration of Fig. 9.5-3. If a fully saturated limit cycle mode is considered, one in which every pulse is saturated, the PWM does not pass perturbations at all. Such a mode is thus stable if the open-loop linear part is stable, and unstable if the open-loop linear part is unstable.

REFERENCES

1. Bergen, A. R.: Discussion of Torng and Meserve (Ref. 26), *IRE Trans. Autom. Control*, vol. AC-5, no. 4 (September, 1960), pp. 304-305.
2. Chow, C. K.: Contactor Servomechanisms Employing Sampled Data, *Trans. AIEE*, pt. II, vol. 73 (March, 1954), pp. 51-61.
3. Da-Chuan, S.: On the Possibility of Certain Types of Oscillations in Sampled-data Control Systems, *Automation and Remote Control*, vol. 20, no. 1 (July, 1959), pp. 77-82.
4. Delfeld, F. R., and G. J. Murphy: Analysis of Pulse-width-modulated Control Systems, *IRE Trans. Autom. Control*, vol. AC-6, no. 3 (September, 1961), pp. 283-292.
5. Dixon, M. V.: Nonlinear Sampled-data System Analysis Using Describing Functions, M.S. thesis, Massachusetts Institute of Technology, Department of Electrical Engineering, Cambridge, Mass., January, 1965.
6. Gocłowski, J. C.: Analysis of a Sampled-data Relay Servo with Hysteresis, *NEREM Record*, 1963.
7. Jury, E. I.: "Sampled-data Control Systems," John Wiley & Sons, Inc., New York, 1958.

8. Jury, E. I., and T. Nishimura: On the Periodic Modes of Oscillation in Pulse-width-modulated Feedback Systems, *Trans. ASME, J. Basic Eng.*, March, 1962, pp. 71-84.
9. Kazakov, V. P.: Study of Pulsed Contactor Automatic Control System Dynamics, *Automation and Remote Control*, vol. 18, no. 1 (April, 1958), pp. 37-49.
10. Kazakov, V. P.: Influence of Hysteresis on the Mode of Periodic Processes in Pulsed Relay Systems, *Automation and Remote Control*, vol. 22, no. 5 (November, 1961), pp. 530-533.
11. Kinnen, I. E., and J. Tou: Analysis of Nonlinear Sampled-data Control Systems, *Trans. AIEE*, pt. II, vol. 78 (January, 1960), pp. 386-394.
12. Korshunov, Y. M.: The Analysis of Periodic States Due to Level Quantization of Signals in Automatic Digital Systems, *Automation and Remote Control*, vol. 22, no. 7 (December, 1961), pp. 778-787.
13. Korshunov, Y. M.: Plotting the Equivalent Complex Amplification Factor of a Nonlinear Pulse Element, *Automation and Remote Control*, vol. 23, no. 5 (November, 1962), pp. 537-547.
14. Kuo, B. C.: The z-transform Describing Function for Nonlinear Sampled-data Control Systems, *Proc. IRE*, vol. 48, no. 5 (May, 1960), pp. 941-942.
15. Kuo, B. C.: "Analysis and Synthesis of Sampled-data Control Systems," Prentice-Hall, Inc., Englewood Cliffs, N.J., 1963.
16. Lepschy, A., and A. Ruberti: The Describing Function for the Study of Sampled-data Control Systems with a Piece-wise Nonlinearity, *Alta Frequenza*, vol. 32 (May, 1963), pp. 357-365.
17. Meserve, W. E., and H. C. Torng: Investigation of Periodic Modes of Sampled-data Control Systems Containing a Saturating Element, *Trans. ASME, J. Basic Eng.*, vol. D-83, no. 1 (March, 1961), pp. 77-81.
18. Nease, R. F.: Analysis and Design of Nonlinear Sampled-data Control Systems, *WADC Tech. Note 57-162, M.I.T. Servomech. Lab.*, June, 1957.
19. Pai, M. A.: Oscillations in Nonlinear Sampled-data Systems, *AIEE Paper CP 62-91*, December, 1961.
20. Pechorina, N. N.: The Stability of Pulse-width Modulated Automatic Control Systems, *Bull. Acad. Sci. U.S.S.R., Power Engineering and Automation*, no. 2, 1960.
21. Pyshkin, I. V.: Limit cycles in Pulse-width Modulated Systems, reprinted in *Theory Appl. Discrete Autom. Systems*, Academy of Sciences of the U.S.S.R., Moscow, 1960, pp. 132-150.
22. Ragazzini, J. R., and G. F. Franklin: "Sampled-data Control Systems," McGraw-Hill Book Company, New York, 1958.
23. Russell, F. A.: Discussion of Chow (Ref. 2), *Trans. AIEE*, pt. II, vol. 73 (March, 1954), pp. 62-64.
24. Simkin, M. M.: The Use of the Describing Function in Nonlinear Pulse Systems, *Automation and Remote Control*, vol. 22, no. 11 (April, 1962), pp. 1345-1353.
25. Torng, H. C.: Complete and Exact Identification of Self-sustained Oscillations in Relay Sampled-data Control Systems, *AIEE Paper CP 62-1059*, May, 1962.
26. Torng, H. C., and W. E. Meserve: Determination of Periodic Modes in Relay Servomechanisms Employing Sampled Data, *IRE Trans. Autom. Control*, vol. AC-5, no. 4 (September, 1960), pp. 298-303.
27. Tou, J. T.: "Digital and Sampled-data Control Systems," McGraw-Hill Book Company, New York, 1959.
28. Tsytkin, Y. Z.: Investigation of Stability of Periodic States in Nonlinear Pulse Automatic Systems, *Automation and Remote Control*, vol. 22, no. 6 (December, 1961), pp. 614-623.

PROBLEMS

- 9-1. Consider the sampled ideal relay shown in Fig. 9-1, with $x(t) = A \sin(\omega t + 45^\circ)$. The t scale has one of the sampling points at its origin. Sketch the waveforms of $x(t)$, $y(t)$, and $y^*(t)$ for several cycles of $x(t)$, in the case $\omega/\omega_s = 1/\pi$. Also indicate on a frequency scale the locations of the harmonic components of $y^*(t)$. What do you conclude about the applicability of describing function theory?

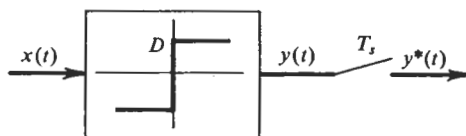


Figure 9-1

- 9-2. Repeat Prob. 9-1 with $\omega/\omega_s = \frac{2}{7}$.
 9-3. Repeat Prob. 9-1 with $\omega/\omega_s = \frac{1}{4}$.
 9-4. (a) For $T_s = 1$ sec, $KD = 10$, $\tau = 3$ sec, find the possible limit cycle modes of the system of Fig. 9-2 and the amplitude of each at $c(t)$.
 (b) What is the general relation between T_s and τ which will ensure that there can be no very large amplitude limit cycle?

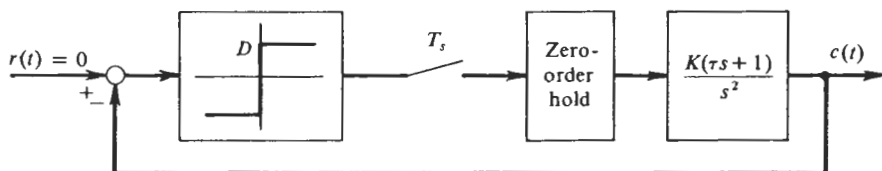
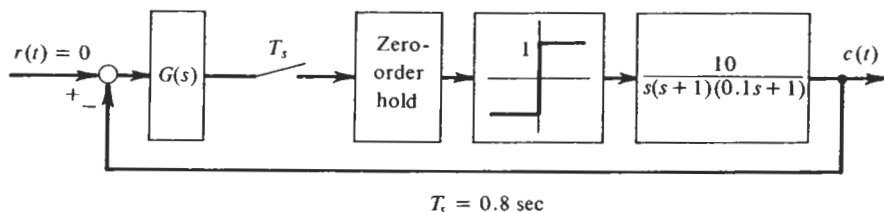


Figure 9-2

- 9-5. What limit cycle modes might the system of Fig. 9-3 display with no compensation, $G(s) = 1$? What is the maximum possible average offset at the output?

Design $G(s)$ so that this system has only the 1, 1 limit cycle mode. What now is the maximum possible average offset at the output? Suggest an additional compensation which will reduce this offset by a factor of 10.



$$T_s = 0.8 \text{ sec}$$

Figure 9-3

- 9-6. Find the maximum permissible relay hysteresis δ such that the system of Fig. 9-4 will display no limit cycle mode of lower frequency than the 3, 3 mode.

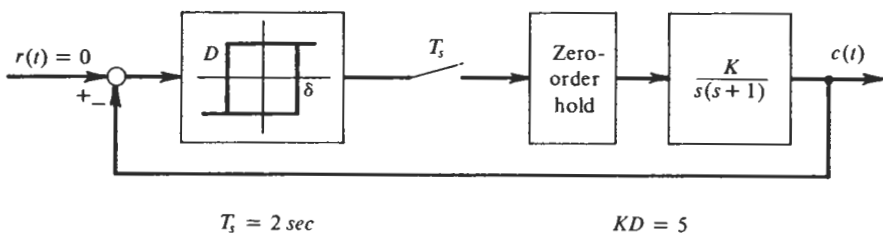


Figure 9-4

- 9-7. Calculate the z-transform describing function for the sampled relay with dead zone for each of the modes shown in Fig. 9.2-8. By comparison with Eqs. (9.2-40), verify in these cases the general relation

$$N^*(A, \varphi) = T_s N(A, \varphi) \quad \omega < \frac{1}{2}\omega_s$$

- 9-8. Use the sampled describing function method as presented in Sec. 9.2 to find the range of τ/T_s for which the 2, 2 limit cycle mode is possible in the system of Fig. 9-5. Interpret your result in terms of the graphical construction suggested for two-level relay systems in Sec. 9.1.

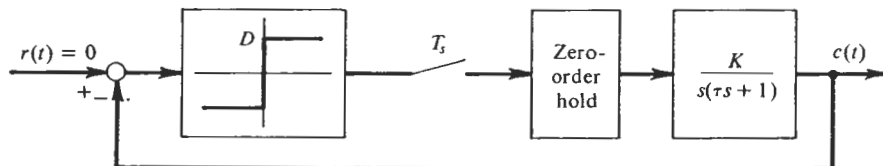


Figure 9-5

- 9-9. Solve Prob. 9-8 using the z-transform describing function method.
- 9-10. For the system of Fig. 9-5, derive the conditions which define the 1, 1 limit cycle mode, using both the sampled and z-transform describing function methods. Note that in this case, where $\omega = \frac{1}{2}\omega_s$, the z-transform describing function method gives a necessary condition, but not sufficient conditions to define the limit cycle.
- 9-11. The system of Fig. 9-6 uses a unit-sensitivity digital lead compensator to stabilize an inertia plant. Use the sampled describing function method to determine the range of τ/T_s which makes the 4, 4 limit cycle mode impossible.

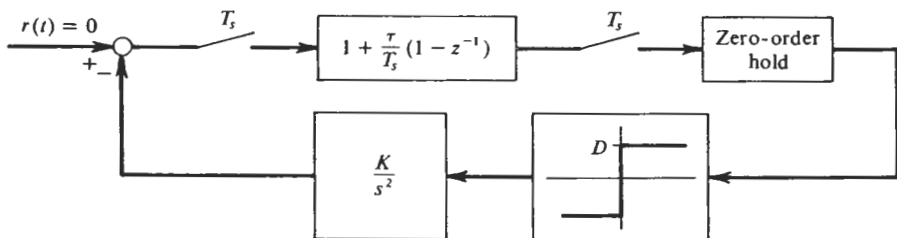


Figure 9-6

- 9-12. Solve Prob. 9-11, using the z-transform describing function method.
 9-13. What is the minimum permissible value of dead zone, δ , which guarantees that the system of Fig. 9-7 will not limit-cycle in the absence of input?

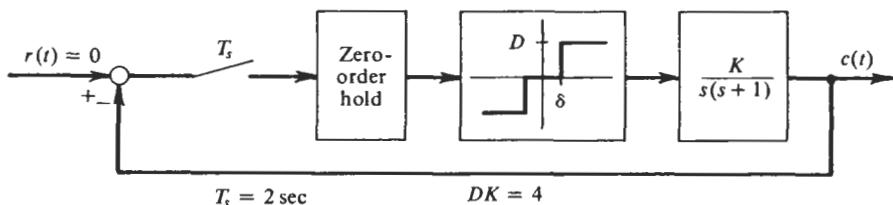


Figure 9-7

- 9-14. If $\delta = 1$, in the system of Fig. 9-7, what limit cycle modes are possible? Suggest a compensation which will eliminate all but the 1, 1 mode.
 9-15. Determine the range of k for which a limit cycle of period $T = 4T_s$, and form $a, 0, -a, 0$ would be stable in the system of Fig. 9-8.

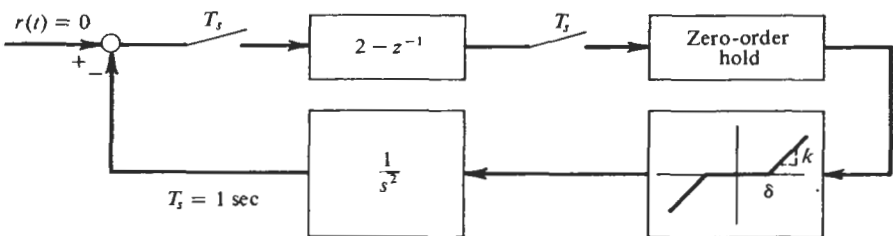


Figure 9-8

- 9-16. Use the difference-equation method to find the exact range of τ/T_s , which makes the 4, 4 limit cycle mode impossible in the system of Fig. 9-6. Compare this result with those given by the describing functions in Probs. 9-11 and 9-12.
 9-17. Repeat Prob. 9-16, using the transform method.
 9-18. What is the maximum gain K that the pulse-width-modulated system of Fig. 9-9 can tolerate without exhibiting any of the limit cycle modes for which the describing function is given in Appendix F? Suggest a compensation which will permit this gain to be doubled without a limit cycle.

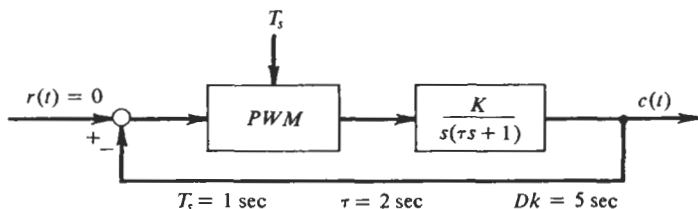


Figure 9-9